Government of India
Ministry of Earth System Sciences (MoES)
India Meteorological Department

REPORT ON FUNNEL-LIKE CLOUD FORMATION OBSERVED IN THE VICINITY OF THOOTHUKUDI AIRPORT AT AROUND 04.45 PM ON 21 JUNE 2026

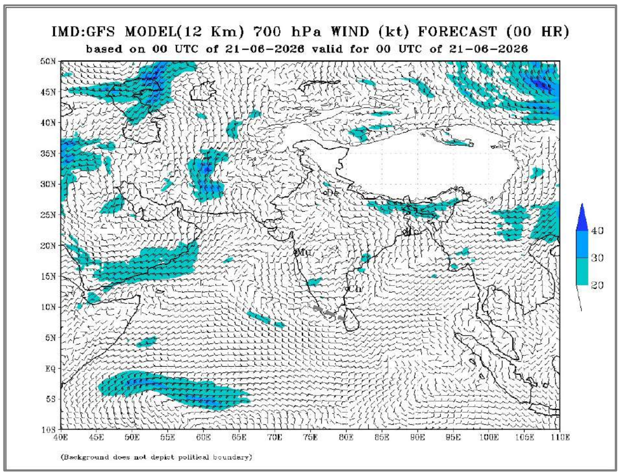

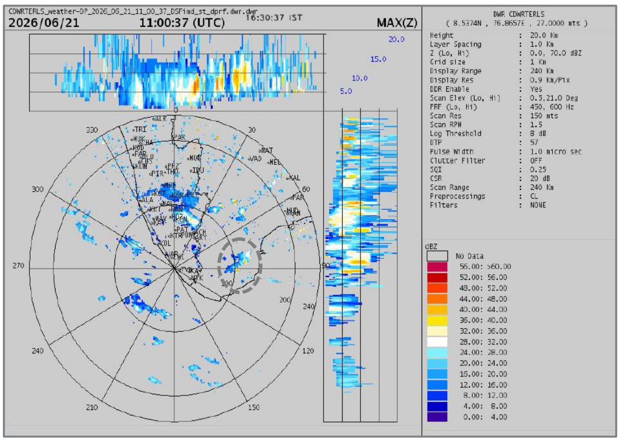

Regional Weather Forecasting Centre,
Regional Meteorological Centre, Chennai
July 2026

Abstract

On **21 June 2026**, a **funnel-like cloud** accompanied by a **rotating dust column** was observed in the vicinity of **Thoothukudi Airport** during a severe convective weather event, prompting an investigation into the possible occurrence of a tornado. This study presents a comprehensive meteorological assessment using **INSAT-3DR satellite imagery, C-band Doppler Weather Radar (DWR), Thiruvananthapuram products (**MAX(Z), PPI(Z), PPI(V), PPI(S), SRI, and HWV), **synoptic weather analysis, airport wind observations, eyewitness reports, photographic evidence, and post-event field damage surveys**.

The analysis indicates that the event developed under the influence of an **east–west trough at the 700 hPa level**, favourable moisture convergence, and atmospheric instability associated with the southwest monsoon, leading to the development of a mature cumulonimbus cloud. Radar observations confirmed a localized severe convective thunderstorm capable of producing strong updrafts, downdrafts, and damaging squally winds. Field investigations documented localized damage to roofs, trees, and utility infrastructure consistent with severe convective winds.

Although a funnel-like cloud and rotating dust column were observed, the available evidence does not support classification of the event as a tornado. Doppler Weather Radar products showed **no hook echo, Tornado Vortex Signature (TVS), mesocyclone, or persistent storm-scale rotation**, while the post-event damage survey revealed **no continuous narrow damage path or convergent damage pattern**, which are key diagnostic characteristics of tornadoes.

The observed meteorological conditions and damage characteristics are most consistent with a **localized severe convective thunderstorm producing damaging squally winds, localized downburst/microburst effects, and a transient gustnado-like circulation** rather than a true tornado. The study highlights the importance of integrating radar observations, satellite imagery, surface meteorological data, and systematic post-event damage surveys for the accurate diagnosis of localized severe weather events and for improving severe weather monitoring and warning services over southern India.

1. Introduction

On 21 June 2026, a funnel-like cloud feature was reported in the vicinity of Thoothukudi Airport at approximately 04:45 PM IST, accompanied by strong winds and a visible dust plume near the surface (Fig. 1a–c). The phenomenon occurred during the passage of an intense convective thunderstorm that affected parts of Thoothukudi district and resulted in localized wind damage to trees, temporary structures, roofing sheets, and other light infrastructure.

The unusual appearance of the funnel-like cloud, together with reports of localized rotation and damaging winds, attracted considerable public attention and raised questions regarding the nature of the phenomenon, including whether it was associated with a tornado or another form of localized convective vortex.

Following the event, a detailed investigation was undertaken utilizing available meteorological observations, Doppler Weather Radar (DWR) products, satellite imagery, surface weather data, eyewitness accounts, photographic and video evidence, and post-event field damage surveys.

The objective of this investigation is to analyze the meteorological conditions, observed impacts, and damage characteristics associated with the funnel-like cloud event reported near Thoothukudi Airport on 21 June 2026. The study seeks to determine the most probable meteorological explanation for the phenomenon through the examination of meteorological observations, Doppler Weather Radar data, satellite imagery, eyewitness reports, photographic and video evidence, and field damage survey findings. The investigation further aims to assess whether the observed feature was associated with a tornado, landspout, gustnado, or other localized convective vortex, and to provide an evidence-based assessment for accurate classification of the event and its associated impacts.

This report presents the findings of the investigation and provides a scientific assessment of the event based on the available meteorological observations and field survey results. The study contributes to a better understanding of localized severe convective weather phenomena over the southern coastal districts of Tamil Nadu and supports future efforts in the monitoring, assessment, and classification of similar high-impact weather events.

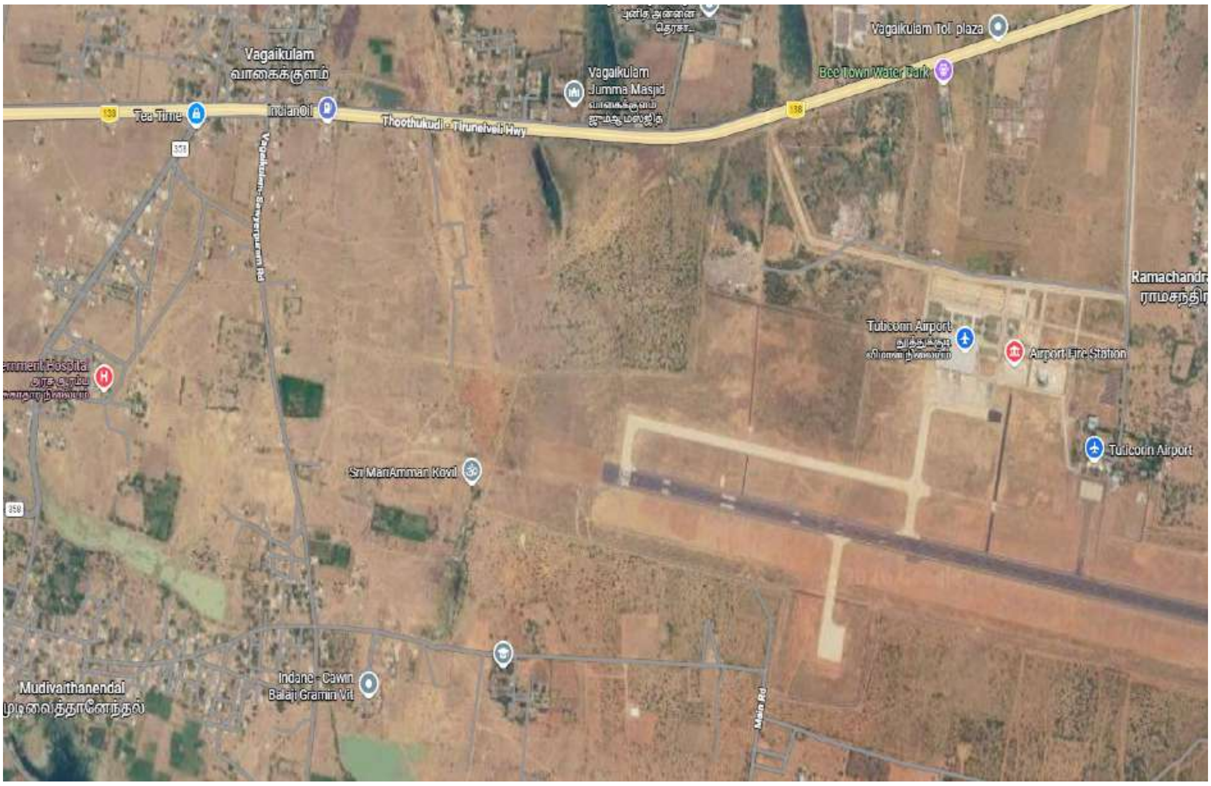

Fig.1a Thoothukudi Airport

Photo Source: IMD official

Fig 1b. Funnel-like cloud feature accompanied by rising dust.

Photo Source: IMD official

Fig. 1c. Funnel-like cloud feature during its **later stage**, accompanied by rising dust

2. Meteorological Situation

Meteorological analysis indicates that thunderstorm activity developed over the Thoothukudi region under the influence of an **east–west trough extending across South Tamil Nadu at the 700 hPa level (approximately 3.1 km above mean sea level)** (**Fig. 2a**). The IMD-GFS 700 hPa wind field shows a zone of cyclonic curvature and low-level convergence over southern Tamil Nadu and adjoining coastal areas, providing favourable dynamical conditions for convective development.

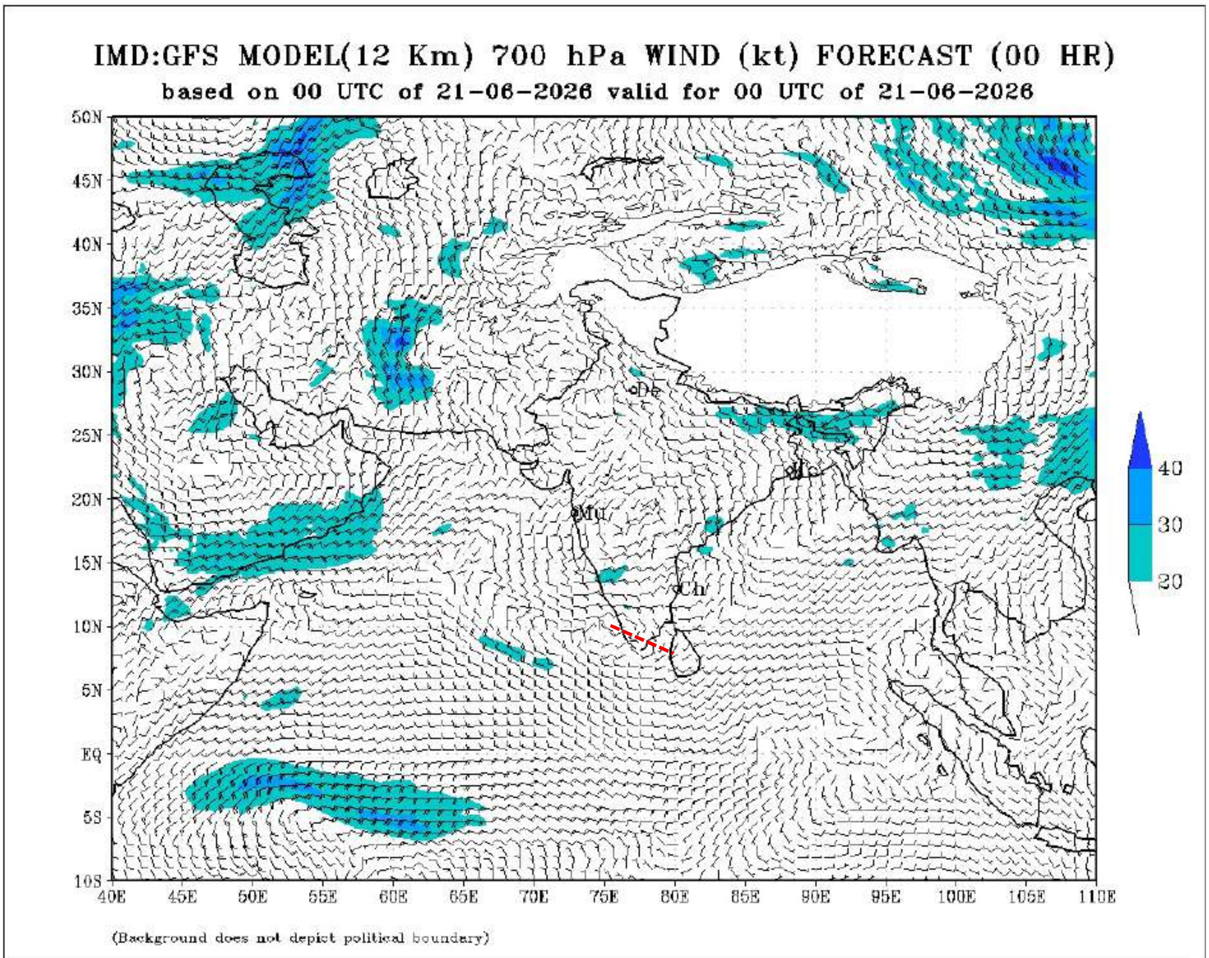

Fig.2a An East-West trough across South Tamil Nadu at 700 hPa

The prevailing atmospheric environment was characterized by adequate moisture availability, instability, and convergence in the lower and middle troposphere. These conditions supported the formation and vertical growth of **deep convective clouds**, which subsequently developed into localized thunderstorms over the Thoothukudi region. The east–west trough acted as a trigger mechanism for sustained upward motion, enhancing convective activity during the afternoon hours.

Under these favourable synoptic and mesoscale conditions, cumulonimbus clouds developed over the area, producing strong updrafts and downdrafts. The associated thunderstorm generated gusty surface winds, localized dust lifting, lightning activity, and short-duration severe weather conditions. The subsequent radar observations and airport wind measurements confirm the presence of an active convective cell capable of producing damaging squally winds over the affected area.

The prevailing atmospheric conditions, characterized by enhanced moisture availability and atmospheric instability, supported the development of deep convective clouds **(Fig. 2b).** These convective systems subsequently evolved into localized thunderstorms accompanied by strong updrafts, gusty surface winds, lightning activity, and localized dust lifting in and around the airport area. Reports and visual observations of a rotating dust column near the airport vicinity suggest the presence of localized low-level rotation within the convective environment. However, based on the currently available evidence, the event is assessed primarily as a severe thunderstorm with damaging squally winds.

2.1 Radar Observation

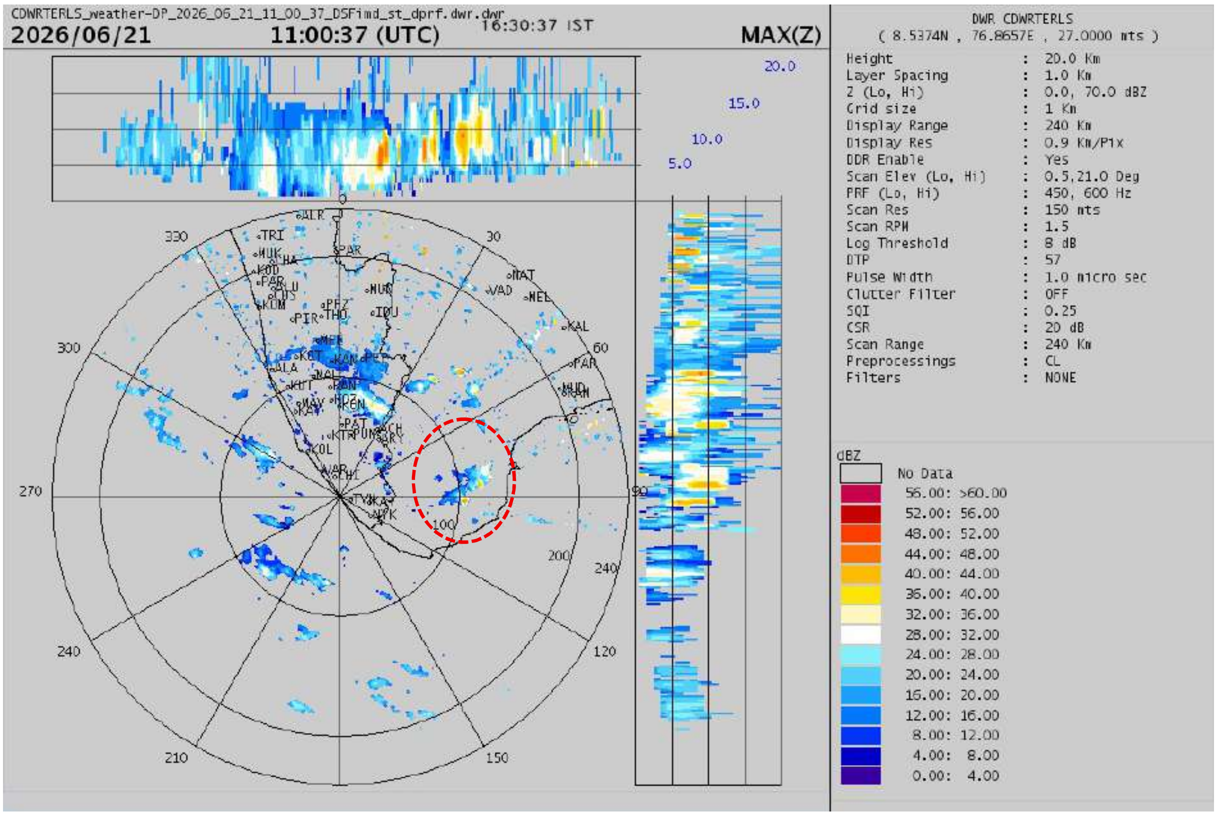

Fig.2b DWR (Trivandrum) Radar image observed at 04.30 PM

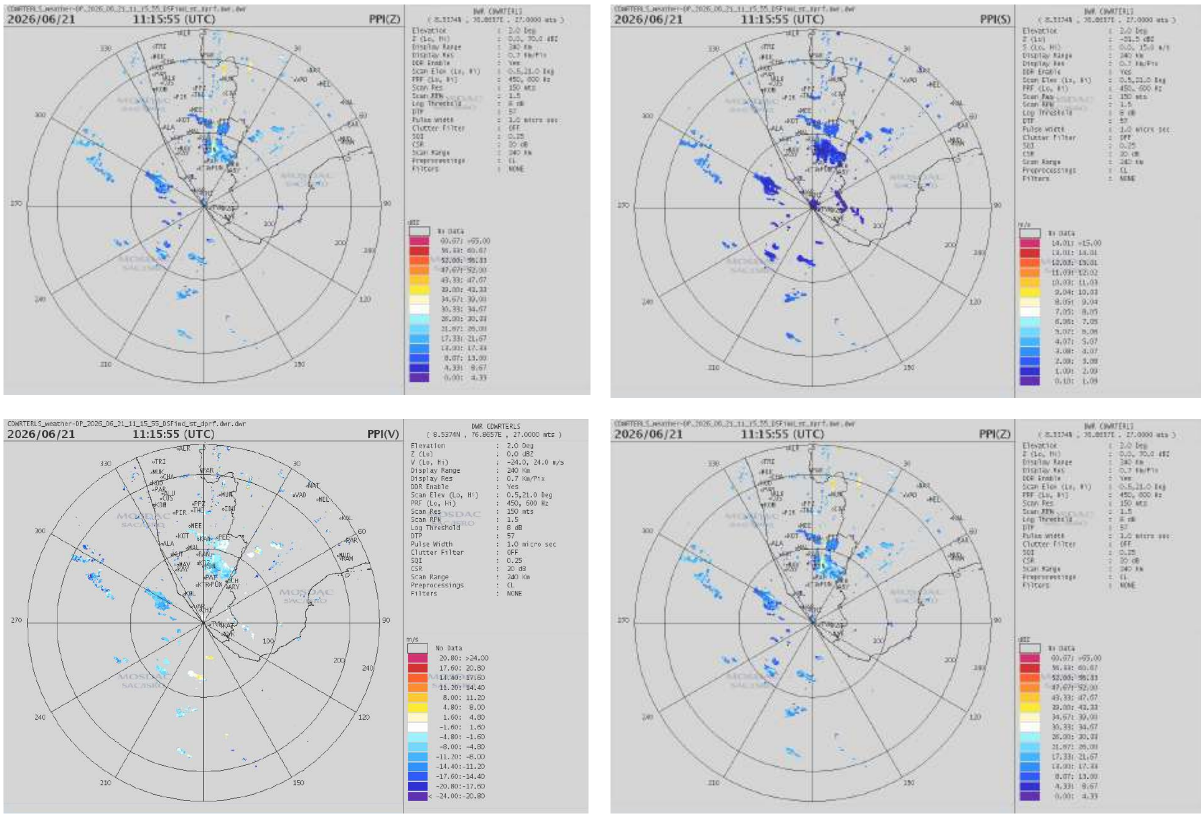

Figure 2c. Doppler Weather Radar (DWR), Thiruvananthapuram, products at **11:15:55 UTC (16:45:55 IST) on 21 June 2026**, comprising **MAX(Z)**, **PPI(Z)**- Plan Position Indicator Reflectivity, **PPI(S)** – Spectrum Width, **PPI(V)** – Radial Velocity

The **Maximum Reflectivity (MAX (Z))** product from the **IMD C-band Doppler Weather Radar (DWR), Thiruvananthapuram**, at **1100 UTC (1630 IST) on 21 June 2026** indicated active convective development over southern Tamil Nadu. A localized area of enhanced radar reflectivity was observed over the **Thoothukudi** region, corresponding closely with the location and timing of the reported severe weather event (**Fig. 2b**). The radar imagery revealed a compact convective cell exhibiting **moderate to strong reflectivity**, indicative of a mature thunderstorm with significant vertical development.

The subsequent radar products acquired at **1115:55 UTC (1645:55 IST)**, including **MAX (Z), PPI(Z), PPI(S), and PPI(V)** (**Fig. 2c**), further confirmed the presence of an active convective storm over the Thoothukudi region. The reflectivity pattern indicated a well-developed cumulonimbus cloud capable of producing strong convective updrafts and downdrafts. The **PPI (V)** product showed localized inbound and outbound radial wind components associated with thunderstorm circulation, while the **PPI(S)** product indicated enhanced spectrum width, suggesting increased turbulence within the storm. The **SRI** product showed localized moderate to heavy rainfall associated with the convective cell. However, none of the radar products exhibited a **hook echo**, **Tornado Vortex Signature (TVS)**, or a well-defined **mesocyclonic circulation**, which are characteristic radar signatures of tornadic thunderstorms.

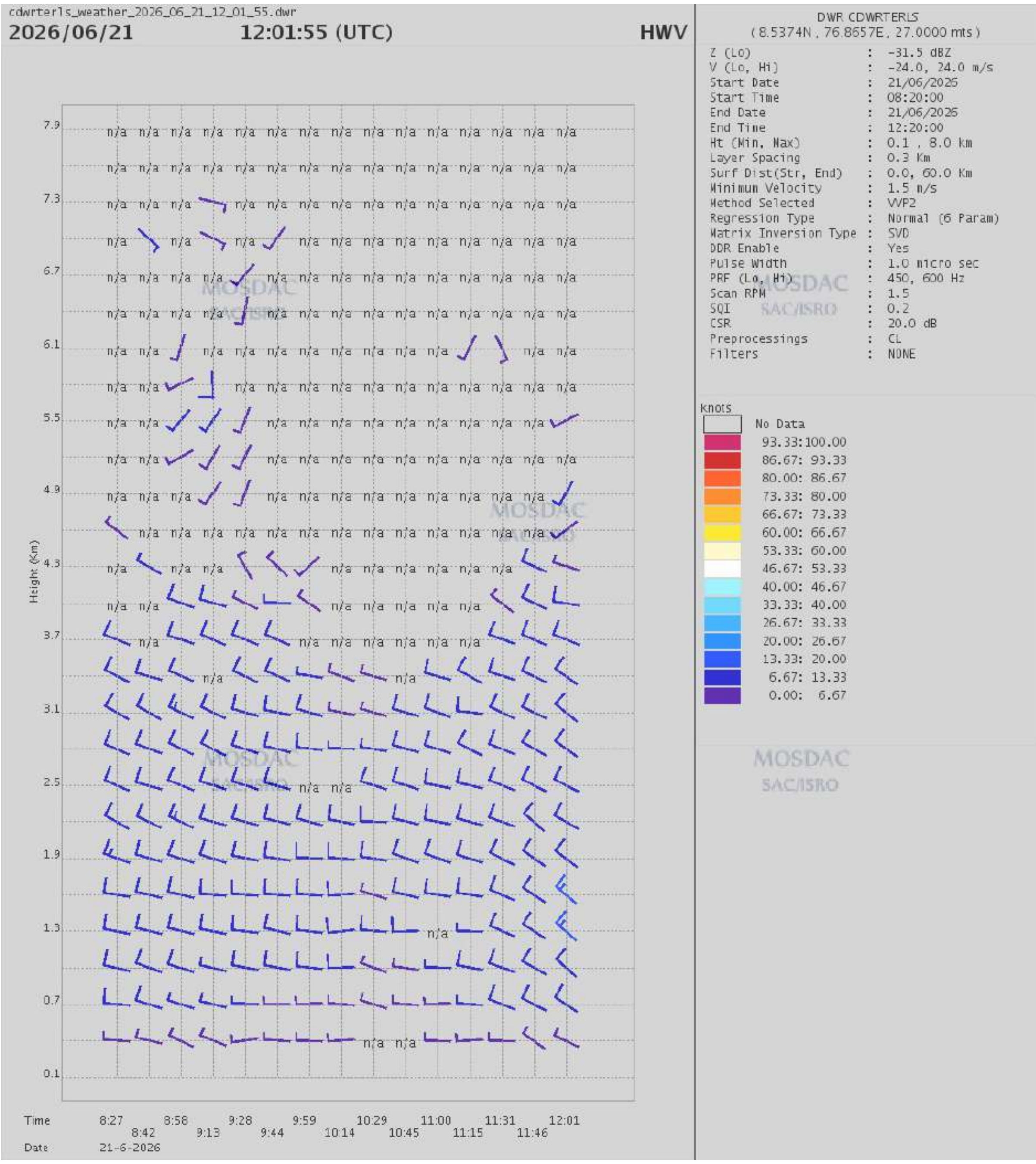

Figure 2d. Height–Wind Vector (HWV) product from the Doppler Weather Radar (DWR), Thiruvananthapuram, **derived from observations between 08:27 and 12:01 UTC (13:57–17:31 IST) on 21 June 2026**

The **Height–Wind Vector (HWV)** product, derived from observations between **0827 and 1201 UTC (1357–1731 IST)** (**Fig. 2d**), showed the prevailing south-westerly monsoon flow with localized wind perturbations associated with the convective storm. Although the HWV product indicated a disturbed wind field during the period of thunderstorm activity, it did not reveal persistent low- to mid-level rotational signatures indicative of organized storm-scale rotation.

The timing of the radar observations closely corresponded with the period of enhanced wind speeds recorded at **Thoothukudi Airport** between **1105 and 1135 UTC (1635–1705 IST)**. The radar signatures are consistent with a localized severe thunderstorm capable of producing strong outflow winds, gust fronts, localized dust lifting, and short-duration severe weather. The combined radar observations, airport wind measurements, and post-event damage survey indicate that the convective cell generated intense downdrafts that reached the surface and spread outward, producing damaging squally winds over the affected area.

Although a **funnel-like cloud** and a **rotating dust column** were observed in the vicinity of **Thoothukudi Airport**, the available meteorological observations and post-event damage survey do not support classification of the event as a **tornado**. The **DWR products (Figs. 2a–2d)** confirmed the presence of a mature convective thunderstorm but showed **no evidence of a hook echo, Tornado Vortex Signature (TVS), mesocyclone, or persistent storm-scale rotation**. Furthermore, the field investigation did not identify a **narrow continuous damage path**, **convergent damage pattern**, or **persistent rotating damage track**, which are the principal diagnostic indicators of tornado occurrence.

The documented damage consisted primarily of roof failures, uprooted trees, broken branches, scattered debris, and damage to utility and public infrastructure. The localized and discontinuous nature of the damage is consistent with **severe thunderstorm outflow winds, localized convective vortices, and possible microburst/downburst activity**, rather than tornadic winds. Accordingly, the integrated analysis of the **DWR observations (Figs. 2a–2d)**, surface meteorological observations, and post-event damage assessment indicates that the event was a **localized severe convective thunderstorm producing damaging squally winds with transient gust-front-induced rotational features (gustnado-like circulation), rather than a confirmed tornado**.

2.2 INSAT-3DR IR IMAGERY

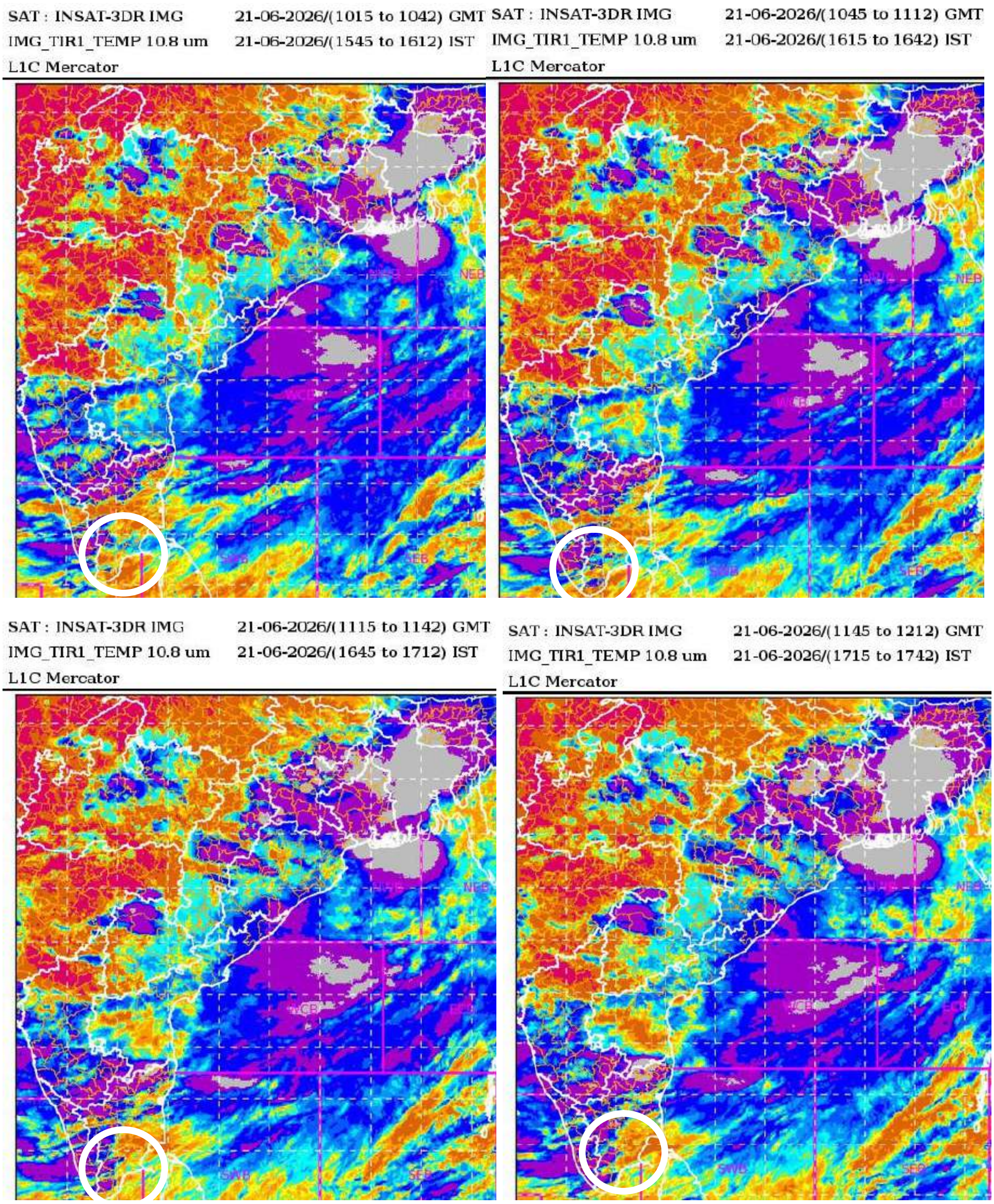

Fig.3a Infrared (IR1, 10.8 µm) imagery: INSAT-3DR 15:45 to 17:42 IST on 21 June 2026

Infrared (IR1, 10.8 µm) imagery from INSAT-3DR acquired between 1545 and 1742 IST on 21 June 2026 (**Fig.3a**) was analyzed to assess the convective activity and thunderstorm potential over Tuticorin district. Successive satellite images revealed the presence of southwest monsoon cloud bands over southern peninsular India and adjoining sea areas. During the observation period, cloudiness gradually increased over Tuticorin district, with scattered convective clouds embedded within the monsoon flow.

The brightness temperature over the district was predominantly in the range of 283–290 K, corresponding to relatively warm cloud tops and indicating moderately developed convective clouds. No extensive areas of very cold cloud tops (<260 K), which are characteristic of deep convective systems and mature cumulonimbus clouds, were observed directly over Tuticorin. Although localized cooling of cloud tops was noticed during the late afternoon, the convection remained disorganized and lacked the vertical extent necessary for severe thunderstorm development.

The satellite imagery indicated locally moderate convective activity associated with moisture incursion from the southwest monsoon. The absence of organized mesoscale convective systems, overshooting tops, and persistent cold cloud tops suggests that any thunderstorm activity over the district was isolated and short-lived. Therefore, based on the evolution of cloud-top brightness temperatures and cloud morphology observed in INSAT-3DR IR imagery, the thunderstorm activity over Tuticorin district on 21 June 2026 can be classified as moderate, with some potential for severe weather.

2.3 Surface Wind Observation at the Thoothukudi Airport

Wind observations at Thoothukudi Airport on 21 June 2026 indicate a short-duration severe wind event associated with a thunderstorm. As shown in **Fig. 3a**, wind speed increased rapidly around 11:05 UTC (16:35 IST) and remained elevated until about 11:35 UTC (17:05 IST), with a peak instantaneous wind speed of 28 knots. During the same period, wind direction exhibited marked fluctuations between approximately 150° and 320° (**Fig. 3b**). The persistence of these directional changes, together with the observation of a funnel-like cloud feature and rising dust, suggests the presence of a localized vortex in the vicinity of the airport.

The observed wind-speed pattern is characteristic of a **severe convective weather event**, typically associated with the passage of a thunderstorm gust front and strong downdraft outflows. During the mature stage of a thunderstorm, precipitation loading and evaporative cooling generate descending air currents that accelerate toward the surface. Upon reaching the ground, these downdrafts spread outward, producing strong and gusty surface winds commonly referred to as squally winds.

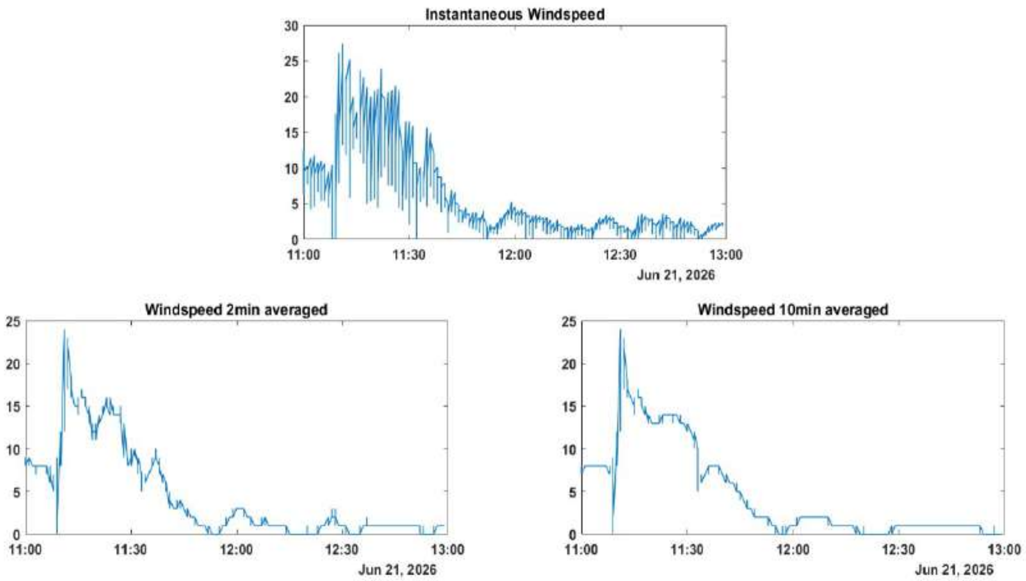

Fig.3a Instantaneous, 2 minutes and 10 minutes average wind Speed observed at Tuticorin Airport during **04.35 PM -05.05PM** [11 -12 UTC] on 21 June 2026

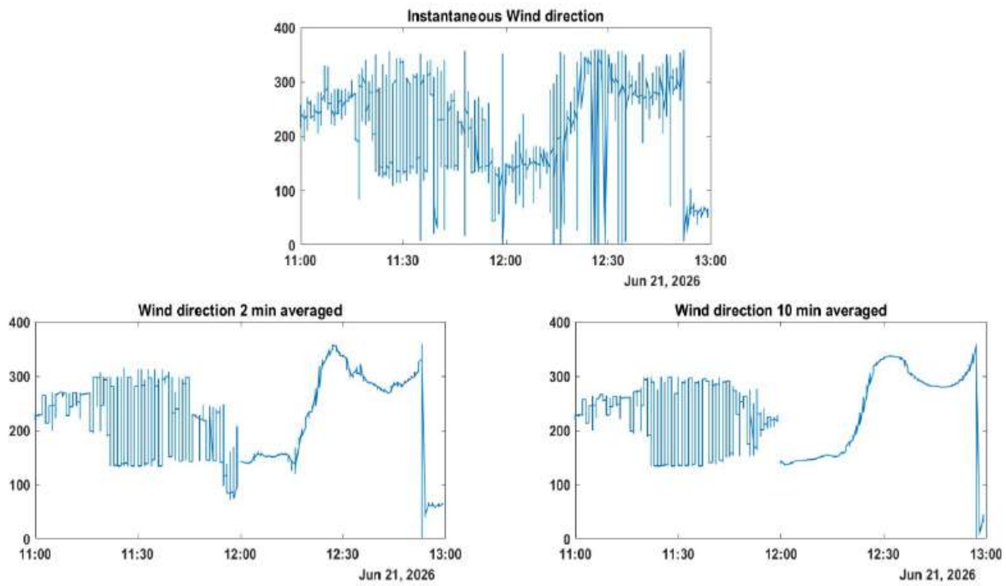

Fig.3b Instantaneous, 2 minutes and 10 minutes average wind Direction observed at Tuticorin Airport during **04.35 PM -05.05PM** [11 -12 UTC] on 21 June 2026

Wind observations recorded at **Thoothukudi Airport** on **21 June 2026** indicate the occurrence of a short-duration severe wind event associated with the passage of a convective thunderstorm. The wind speed increased rapidly between **1105 and 1135 UTC (1635–1705 IST)**, reaching a peak instantaneous wind speed of approximately **28 knots**, before gradually decreasing. This temporal variation is characteristic of the passage of a **thunderstorm outflow boundary (gust front)** generated by strong downdrafts within a mature cumulonimbus cloud. Such outflow winds are capable of producing localized damage to lightweight structures, roofing materials, vegetation, and utility infrastructure.

As shown in **Fig. 3b**, the wind direction exhibited pronounced variability between approximately **1110 and 1150 UTC**, fluctuating repeatedly between **150° and 320°**. These rapid directional changes, observed in both the instantaneous and 2-minute averaged wind records, indicate a highly turbulent convective wind field. This period coincided with eyewitness reports of a **funnel-like cloud** and a **rising dust column** near the **Vagaikulam–Thoothukudi Airport** area, suggesting the presence of a localized transient vortex embedded within the thunderstorm outflow. The observed wind characteristics are consistent with thunderstorm-induced downdrafts, gust-front passage, and localized rotational features commonly associated with severe convective storms.

A post-event field survey documented damage to residential buildings, commercial establishments, utility infrastructure, vegetation, and transportation facilities. The observed damage included removal of roof tiles and corrugated roofing sheets, damage to lightweight and temporary structures, uprooted trees, broken branches, damaged signboards, and scattered debris. These impacts are typical of severe convective winds and indicate that wind intensity varied considerably across the affected area.

Comparison of the observed damage with the **Beaufort Wind Scale** suggests that the maximum wind intensity over the most severely affected locations was approximately **Beaufort Force 9–10 (Strong Gale to Storm)**, corresponding to sustained wind speeds of about **41–55 knots (76–102 km h^{-1})**. Since structural damage is primarily governed by **peak gusts** rather than sustained winds, localized maximum gusts were estimated using a typical convective thunderstorm gust factor of **1.3–1.5**. Accordingly, **peak gusts in the most severely affected locations are estimated to have locally exceeded 60 knots**

(approximately 110 km h^{-1}). These estimates are based on the observed damage characteristics and represent localized peak wind conditions that were not necessarily captured by the airport anemometer.

The combined analysis of airport wind observations and post-event damage assessment indicates that the severe weather event was dominated by **intense localized convective winds associated with a mature thunderstorm**. The sudden increase in wind speed, rapid directional changes, localized damage pattern, and evidence of transient rotation is consistent with strong thunderstorm outflow, localized convective vortices, and possible gust-front-induced circulation. Overall, the observations support the interpretation that the event was a **localized severe convective thunderstorm producing damaging squally winds and transient rotational features**, rather than a widespread synoptic wind event.

3. Photographic Evidence and Event Evolution

A sequence of photographs obtained from the vicinity of **Thoothukudi Airport (Vagaikulam)** provides valuable visual documentation of the development, intensification, and dissipation of the severe weather event that occurred on **21 June 2026**. The photographs capture the evolution of a mature thunderstorm and the subsequent formation of a prominent rotating dust vortex in the airport vicinity. The sequence also provides important contextual evidence regarding the prevailing environmental conditions and the interaction between the thunderstorm outflow and the local surface environment.

Stage 1 – Thunderstorm Development (Figure 4a)

Figure 4a shows a well-developed cumulonimbus cloud over the airport area during the mature stage of thunderstorm evolution. The cloud exhibits significant vertical development with a pronounced precipitation shaft visible on the western side of the storm. The cloud base appears relatively low and irregular, with localized lowering beneath the main convective tower.

The observed cloud structure is characteristic of an active convective storm containing strong updrafts and downdrafts. The extensive vertical growth of the cloud indicates substantial atmospheric instability and moisture availability, while the precipitation shaft suggests the presence of intense downdraft activity. Such thunderstorms are capable of generating strong surface wind gusts, gust fronts, and localized severe weather phenomena.

The appearance of the storm in Figure 4a represents the initial stage of the event prior to the development of the visible dust vortex. At this stage, the thunderstorm had already attained sufficient intensity to produce strong outflow winds over the surrounding area

Photo Source: IMD official

Figure 4a. Well-developed cumulonimbus cloud over the Thoothukudi Airport area prior to vortex formation**.**

Stage 2 – Dust Vortex Formation (Figures 4b and 4c)

Figure 4b captures the initial development of a concentrated dust column beneath the thunderstorm cloud base. The dust plume appears vertically developed and well organized, extending upward from the surface into the lower atmosphere. The structure indicates strong low-level convergence, vigorous upward motion, and localized rotation within the thunderstorm outflow environment.

Photo Source: IMD official

Figure 4b. Initial formation of a concentrated dust column beneath the thunderstorm cloud base near Vagaikulam, Thoothukudi

At the time of the event, major highway expansion works were underway along the **Tirunelveli–Thoothukudi National Highway** near the **Vagaikulam area**. Large quantities of loose red soil had been excavated and stockpiled adjacent to the construction corridor for embankment and road-laying activities. These unconsolidated soil deposits provided an abundant source of fine particulate material that could be readily lifted by strong winds.

As the thunderstorm outflow intensified, the localized vortex entrained substantial quantities of this loose red soil and transported it upward, producing the prominent dust column visible in the photograph. The availability of exposed construction material significantly enhanced the visibility of the vortex, making the circulation readily observable from the airport area and surrounding locations.

Photo Source: IMD official

Figure 4c. Vortex observed near the *Thoothukudi Airport*.

The concentration of airborne dust and debris indicates that the vortex possessed sufficient intensity to entrain and transport large quantities of loose surface material. The narrow and vertically organized structure of the dust column suggests the presence of a **localized rotating circulation embedded within the thunderstorm outflow** boundary. The simultaneous occurrence of strong thunderstorm activity aloft and organized dust lifting at the surface indicates a direct interaction between the convective storm and the local surface environment.

Stage 3 – Maximum Intensity (Figures 4d and 4e)

Figure 4d captures the vortex during its most organized and visually prominent stage. A distinct lowering beneath the cloud base is visible directly above the dust column, while the vortex itself appears denser and more vertically continuous than in the earlier stages.

The photograph suggests a period of maximum interaction between the thunderstorm circulation and the surface-based vortex. The large volume of suspended dust indicates intense near-surface winds capable of lifting and maintaining significant quantities of particulate matter within the circulation.

The cloud-base lowering observed in the image is noteworthy because it indicates enhanced vertical motion in the immediate vicinity of the vortex. However, the photograph does not conclusively demonstrate the existence of a continuous condensation funnel extending from the cloud base to the surface.

Photo Source: IMD official

Figure 4d. Vortex at its peak organization beneath the thunderstorm cloud base in the vicinity of *Thoothukudi Airport*,

Photo Source: IMD official

Figure 4e Mature Dust Column and Ongoing Soil Entrainment near the Airport

The intensity of the dust lifting observed in this image suggests that the vortex coincided with the period of strongest winds recorded at Thoothukudi Airport. Airport observations indicate peak wind speeds approaching **28 knots** during this phase of the event.

The photographs demonstrate that the circulation remained highly localized, with the most intense dust lifting concentrated within a relatively narrow area. Such characteristics are commonly observed in gust-front vortices, gustnadoes, and weak landspout-type circulations. Overall, Figures 4d and 4e represent the peak intensity phase of the event, during which the vortex was most organized and visually prominent.

Stage 4 – Dissipation (Figure 4f)

Photo Source: IMD official

Figure 4f. Dissipation stage of the dust vortex with residual suspended dust and thunderstorm outflow winds

Figure 4f depicts the weakening stage of the event. The previously concentrated dust column is no longer visible as a discrete feature, having dispersed into a broader area of suspended dust and haze.

Although strong winds remain evident from the continuing movement of dust and vegetation, the organized circulation appears to have weakened substantially. The airborne dust becomes more diffuse and widespread, indicating a transition from a localized vortex to broader thunderstorm outflow winds.

The cloud base remains active, suggesting that the parent thunderstorm had not completely dissipated. However, the localized circulation responsible for the prominent dust column had largely collapsed by this stage. The photograph therefore represents the final stage of the event, characterized by residual strong winds, widespread dust suspension, and gradual weakening of the convective circulation over the airport area.

The available photographic evidence, supported by meteorological observations, airport wind measurements, and Doppler Weather Radar imagery, indicates that the weather event affecting the **Thoothukudi Airport (Vagaikulam) area on 21 June 2026** was associated with a severe convective thunderstorm capable of producing strong updrafts, downdrafts, and damaging outflow winds. The photographic sequence clearly documents the evolution of the event, from the development of a mature cumulonimbus cloud to the formation, intensification, and eventual dissipation of a prominent rotating dust vortex in the vicinity of the airport.

The occurrence of the vortex coincided with a period of enhanced wind speeds observed at Thoothukudi Airport and the presence of an active convective cell identified in Doppler Weather Radar observations from DWR Thiruvananthapuram. The visibility and prominence of the dust vortex were further enhanced by the availability of large quantities of loose red soil associated with ongoing highway expansion works near Vagaikulam, which were readily entrained and lifted into the atmosphere by the strong winds.

The photographic evidence demonstrates a well-defined rotating dust column beneath the thunderstorm cloud base, indicating strong low-level convergence, vigorous upward motion, and localized rotation. However, the available imagery does not conclusively show a continuous condensation funnel extending from the cloud base to the ground, nor does it provide sufficient evidence to establish a persistent cloud-to-surface circulation characteristic of a tornado.

Based on the currently available meteorological, radar, wind, and photographic evidence, the observed phenomenon is assessed as being **most consistent with a localized rotating dust vortex associated with severe thunderstorm outflow**. While a **landspout-type vortex** cannot be completely ruled out, there is insufficient evidence at present to confirm the occurrence of a tornado. Accordingly, the event is best classified as a **severe thunderstorm accompanied by damaging squally winds and a localized rotating dust vortex.**

3. Significant impacts

A severe thunderstorm accompanied by strong squally winds affected parts of Thoothukudi district during the evening hours of 21 June 2026. The event produced damaging winds that resulted in localized but significant impacts to residential structures, commercial facilities, and public infrastructure. Field photographs and preliminary assessments indicate widespread roof damage, structural impacts to buildings, and damage to roadside facilities. The overall damage pattern is consistent with severe convective wind activity associated with an intense thunderstorm.

3.1 Areas Affected and Observed Damage

Based on available reports, field observations, and photographic evidence, the most affected locations were:

a) Mudivaithanendal

b) Vagaikulam Toll Plaza facilities

c) A private amusement/theme park near Thoothukudi Airport

The following impacts were documented during the field survey:

a) Extensive roof damage to residential buildings at Mudivaithanendal, including the loss of roofing sheets, displacement of roof tiles, and partial roof collapse.

b) Damage to the Vagaikulam Toll Plaza infrastructure, including roofing components and associated facilities located near Thoothukudi Airport.

c) Damage to a private amusement/theme park facility in the vicinity of Thoothukudi Airport, including impacts to lightweight structures and associated installations.

d) Scattering and displacement of loose materials and debris, indicative of strong localized wind gusts.

e) No evidence of complete building collapse was observed in any of the surveyed locations.

The observed damage was generally localized and discontinuous in nature, with impacts concentrated on exposed and lightweight structures. The damage characteristics are consistent with severe thunderstorm outflow winds and localized downburst/microburst activity.

A severe thunderstorm accompanied by strong squally winds affected parts of Thoothukudi district during the evening hours of 21 June 2026. The event produced damaging winds that resulted in localized but significant impacts to residential structures, commercial facilities, and public infrastructure. Field photographs and preliminary assessments indicate a few roof damage, and damage to roadside facilities. The damage pattern is consistent with severe convective wind activity associated with an intense thunderstorm.

PHOTOGRAPHIC EVIDENCE: MUDIVAITHANENDAL

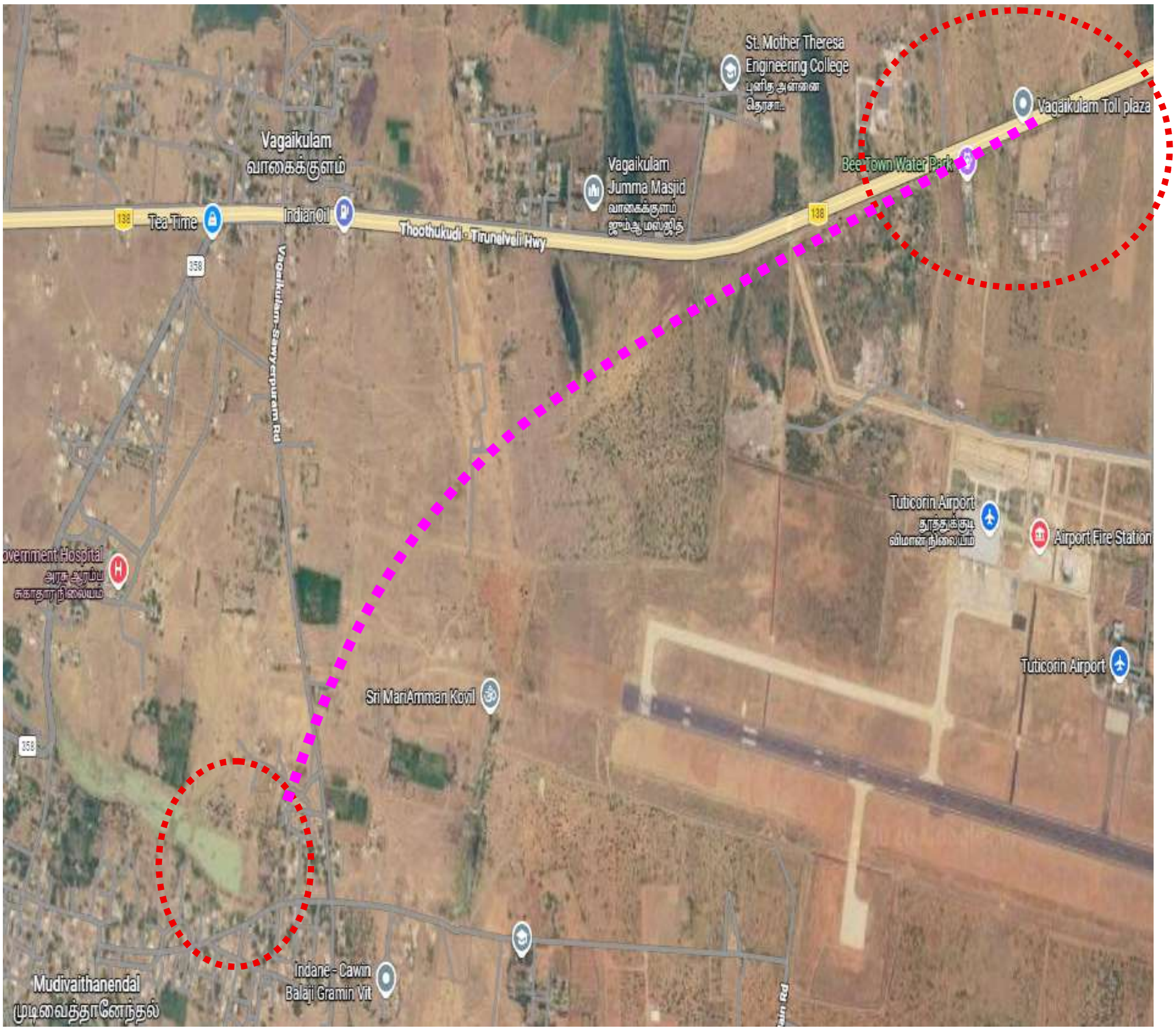

Photo Source: IMD official

Fig 5a. The track of Cb cloud from Mudivaithanendal village to Vagaikulam Toll Plaza,

Photo Source: IMD official

Fig 5b. Inspection at Mudivaithanendal residential buildings

Field Investigation and Data Collection

Following the event, officials from the India Meteorological Department (IMD) conducted a detailed field inspection of the affected areas to assess the nature and extent of the damage. The inspection covered Mudivaithanendal village, Vagaikulam Toll Plaza, the Water Theme Park near Vagaikulam, and areas extending towards Thoothukudi Airport. Particular attention was given to damage sustained by residential buildings, including the loss of roof tiles and roofing sheets, damage to temporary structures, and impacts on vegetation and other exposed infrastructure.

During the field survey, photographic evidence of the damage was systematically documented, and eyewitness accounts of the incident were collected from residents and affected persons in the surveyed locations. Information regarding the timing of the event, observed weather conditions, wind characteristics, visible cloud features, and damage occurrence was obtained through interactions with local residents and stakeholders. The photographic documentation and eyewitness testimonies collected during the field investigation formed an important component of the assessment and were used in conjunction with meteorological observations, radar data, satellite imagery, and damage survey findings to evaluate the nature of the event and determine its most probable meteorological classification.

Photo Source: IMD official

Photographic evidence documenting the loss of roof tiles and roof damage to residential buildings at Mudivaithanendal village, along with damage observed at other surveyed locations, is appended in Annexure-I.

4. Post-Event Damage Survey and Assessment

A post-event assessment was carried out based on field observations, photographic evidence, eyewitness accounts, airport meteorological observations, and Doppler Weather Radar data. The damage was concentrated along a corridor extending from **Mudivaithanendal village towards Vagaikulam and the Thoothukudi Airport vicinity**, suggesting the passage of a localized severe wind event. The affected locations included residential areas, the Vagaikulam Toll Plaza, a private amusement/theme park, and areas adjacent to the airport.

The most significant damage was observed in **Mudivaithanendal village**, where several residential structures suffered partial roof failures, including the removal of roof tiles and roofing sheets. In many instances, roof materials were displaced and thrown away from their original locations, exposing portions of the interior living spaces. Photographic evidence indicates extensive roof tile loss affecting multiple houses, while the structural walls of the buildings generally remained intact, suggesting that the damage was primarily wind-related rather than due to structural collapse.

Damage was also reported at the **Vagaikulam Toll Plaza**, where roofing elements and associated structures sustained wind-related impacts. Similarly, a nearby private amusement/theme park experienced damage to roof coverings and lightweight structures. No evidence of complete building collapse was reported from any of the affected locations.

Eyewitness accounts provide additional insight into the nature of the event. Residents of Mudivaithanendal reported that roof tiles were lifted and thrown predominantly toward the western side of affected houses, while nearby trees exhibited broken branches rather than widespread uprooting. Witnesses further reported the sudden onset of strong winds around **1630 IST**, resulting in the removal of roofing materials from residential buildings. In the Vagaikulam area, eyewitnesses described a strong rotating wind that damaged portions of the Toll Plaza roof and nearby amusement park structures. A separate observer reported seeing a funnel-like cloud feature accompanied by rising dust near Thoothukudi Airport around **1700 IST**.

The damage pattern indicates the occurrence of **intense localized wind gusts**, with impacts concentrated mainly on roofing systems, lightweight structures, and exposed facilities. The absence of complete structural collapse, widespread tree uprooting, or catastrophic damage suggests that the event was of relatively limited spatial extent and duration. Utility services experienced localized disruptions, and transportation routes were temporarily affected by debris and fallen branches.

From a meteorological perspective, the observed damage is consistent with a **severe thunderstorm producing strong squally winds and localized enhanced wind circulation**. The combination of radar observations, airport wind measurements, photographic evidence of a rotating dust vortex, and eyewitness reports suggests that the damaging winds were associated with thunderstorm outflow. The concentration of damage along a relatively narrow corridor and reports of localized rotation indicate the possibility of a **landspout-type vortex embedded within the thunderstorm outflow**. However, the currently available evidence does not conclusively establish the presence of a tornado, as a continuous damage path, convergent damage pattern, and Doppler radar velocity signatures confirming tornadic circulation have not been documented.

Overall, the post-event assessment indicates that the damage was caused by a **localized severe convective wind event associated with a thunderstorm**, producing damaging strong winds and a rotating dust vortex. Based on the available evidence, the event is assessed as being **most consistent with localized thunderstorm-induced land spout-type vortex**.

5. Thermodynamic Environment

The thermodynamic environment evaluated using numerical weather prediction model analyses (ECMWF). The atmospheric stability indices derived from the **ERA5 reanalysis** and averaged over the grid points 8.50°–8.825° N and 78.00°–78.25° E for the period 21 June 2026 (1600–1800 IST) (**Table 1 & Fig 6a**) indicate that the thermodynamic environment over Tuticorin Airport was highly conducive to thunderstorm development.

The atmospheric stability indices indicate that the environment over **Tuticorin Airport** was favourable for the development of thunderstorms. The **Convective Available Potential Energy (CAPE)** of **1242 J kg⁻¹** suggests a moderately unstable atmosphere capable of supporting deep convection. Although a **Convective Inhibition (CIN)** of **−48.9 J kg⁻¹** indicates the presence of a weak to moderate capping layer, this level of inhibition can be readily overcome by surface heating or mesoscale lifting mechanisms such as sea-breeze convergence.

The **K Index** of **35.0°C** (**Table 1 & Fig 6a**) indicates a high probability of thunderstorm occurrence, while the **Total Totals Index** of **44.6°C** further confirms the presence of favourable thermodynamic conditions for convective development. The **Showalter Index** (**−0.5°C**) and **Lifted Index** (**−3.16°C**) are both negative, indicating atmospheric instability and the potential for sustained convective updrafts.

The **precipitable water** value of **54.5 mm** reflects a highly moist atmospheric column, providing sufficient moisture to support deep convective clouds and efficient precipitation processes. Consequently, any thunderstorms developing over the region would be capable of producing **heavy rainfall, frequent lightning, and localized gusty winds**.

Table 1. ERA5 reanalysis data averaged over Lat 8.50°–8.825° N, Long 78.00°–78.25° E during 1600–1800 IST on 21 June 2026.

PARAMETER	**VALUES**
CAPE	**1242.05 J/ KG**
CIN	**-48.92 J/ KG**
K_INDEX	**35.04 °C**
TOTAL_TOTALS_INDEX	**44.61 Δ°C**
PRECIPITABLE WATER	**54.54 MM**
SHOWALTER_INDEX	**-0.51 Δ°C**
Lifted Index	**-3.16 Δ°C**

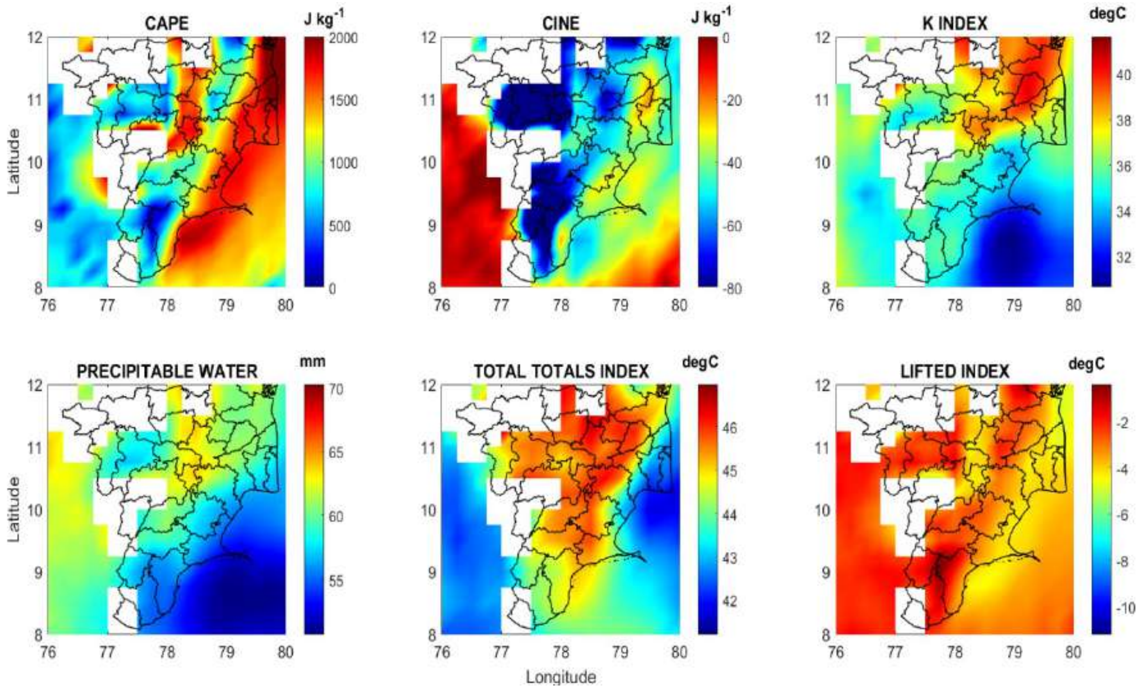

Figure 6a. Thermodynamic indices over the Thoothukudi region derived from ERA5 reanalysis (1600–1800 IST, 21 June 2026)

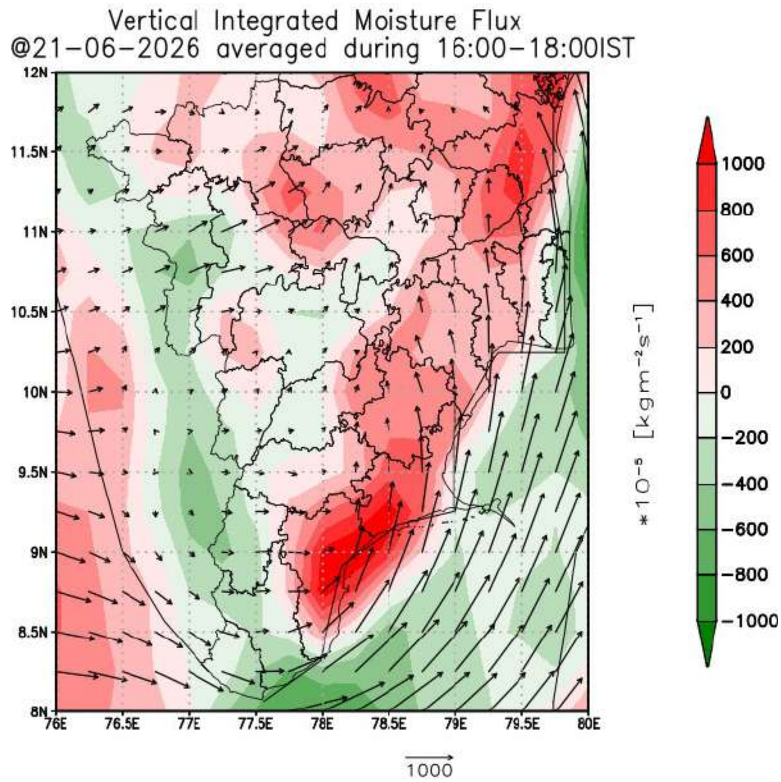

Figure 6b. VIMFC over the Thoothukudi region derived from ERA5 reanalysis (1600–1800 IST, 21 June 2026)

The **Vertically Integrated Moisture Flux Convergence (VIMFC)** averaged during **1600–1800 IST on 21 June 2026** (**Fig. 6b**) indicates **strong positive moisture convergence** over the **Thoothukudi–Vagaikulam region**. The enhanced low-level moisture convergence provided a favourable environment for the rapid development and intensification of deep convection, supporting the formation of a mature cumulonimbus cloud capable of producing strong updrafts, damaging squally winds, and the observed funnel-like cloud.

Overall, the combined stability indices suggest that the atmosphere over Tuticorin Airport was **moderately unstable and highly conducive to thunderstorm development**. While the thermodynamic conditions strongly favoured convective initiation and precipitation, the occurrence and intensity of thunderstorms would also depend on the availability of dynamic forcing mechanisms, such as low-level convergence, sea-breeze interactions.

6. Diagnostic Assessment of the Funnel-like Feature

Based on meteorological observations, Doppler Weather Radar (DWR) analysis, satellite imagery, eyewitness reports, visual documentation, and post-event field survey findings, the severe weather event that affected parts of Thoothukudi district on 21 June 2026 was associated with an intense convective thunderstorm that developed within the southwest monsoon environment. The storm formed under favourable conditions characterized by enhanced low-level moisture convergence, strong daytime heating, and an east–west trough at the 700 hPa level.

6.1 Severe Thunderstorm Outflow Winds

The primary cause of the observed damage was most likely strong thunderstorm outflow winds generated by a mature cumulonimbus cloud. Intense downdrafts transported cooler air from higher levels of the atmosphere toward the surface. Upon reaching the ground, the descending air spread outward rapidly, producing strong gust fronts and squally winds capable of causing structural damage.

The observed impacts, including roof damage, displacement of roofing materials, damage to lightweight structures, and the scattering of loose debris, are consistent with severe thunderstorm outflow winds.

6.2 Localized Microburst/Downburst Activity

The concentration of damage in certain locations suggests that portions of the thunderstorm may have produced localized microburst or downburst activity. These phenomena occur when a concentrated column of descending air reaches the surface and spreads outward, generating intense straight-line winds over a relatively small area.

Evidence supporting this assessment includes:

- Sudden onset of strong winds.
- Localized areas of more severe damage.
- Discontinuous distribution of damage.
- Damage characteristics consistent with intense straight-line winds.

Localized microburst/downburst activity likely contributed to the enhanced damage observed in some affected areas.

6.3 Tornado Assessment

Table. 2 Tornado Criteria versus Observations

Diagnostic Parameter	Typical Tornado	Observation during Thoothukudi Event	Assessment
Funnel-like cloud	Yes	Observed	✓
Dust/debris column	Yes	Observed	✓
Narrow continuous damage path	Present	Not observed	✗
Convergent damage pattern	Present	Not observed	✗
Persistent rotating damage track	Present	Not observed	✗
Tornado Vortex Signature (TVS)	Usually, present	Not observed	✗

Persistent storm-scale rotation	Usually, present	Not observed	✗
Hook echo	Often present	Not identified	✗
Localized severe damage	Yes	Not observed	✗
Severe convective thunderstorm	Yes	Observed	✓

Although a funnel-like cloud and a rotating dust column were observed in the vicinity of Thoothukudi Airport, the available meteorological observations and post-event damage survey **do not support classification of the event as a tornado**. The investigation found **no evidence of a narrow, continuous damage path, convergent damage pattern, persistent rotating damage track, hook echo, Tornado Vortex Signature (TVS), or organized storm-scale rotation**, which are key diagnostic indicators of tornado occurrence.

The documented damage consisted primarily of roof failures, uprooted trees, scattered debris, and damage to utility and public infrastructure. These impacts were localized and discontinuous and are consistent with **severe thunderstorm outflow winds, localized convective vortices, and possible microburst/downburst activity**, rather than tornadic winds.

Accordingly, based on the available satellite observations, radar reflectivity data, surface wind measurements, eyewitness reports, and detailed post-event damage assessment, the event is best classified as a localized severe thunderstorm producing damaging squally winds with transient rotational features, rather than a confirmed tornado event.

6.4 Gustnado Assessment

The observed meteorological conditions, radar signatures, surface wind observations, and post-event damage characteristics were compared with the documented characteristics of a typical gustnado. A gustnado is a shallow, short-lived vortex that develops along the gust front of a severe thunderstorm and is not associated with a mesocyclone or persistent storm-scale rotation.

Table 3. Comparison of Gustnado Characteristics with Observations

Characteristic	Typical Gustnado Characteristics	Observations during the Thoothukudi Event	Assessment
Parent storm	Develops along the gust front of a severe thunderstorm	Occurred during an intense convective thunderstorm	Consistent
Thunderstorm outflow	Associated with strong outflow/gust front	Strong squally winds and rapidly changing wind direction observed	Consistent
Dust/debris column	Visible rotating dust column commonly observed	Prominent dust column observed near Vagaikulam–Thoothukudi Airport	Consistent
Funnel-like cloud	May occur beneath the cumulonimbus cloud	Funnel-like cloud observed beneath the Cb cloud	Consistent
Duration	Short-lived (typically a few minutes)	Feature persisted briefly during the thunderstorm	Consistent
Spatial extent	Highly localized	Damage confined mainly to the Vagaikulam–Thoothukudi Airport sector	Consistent
Damage pattern	Localized and discontinuous	Damage restricted to isolated locations with no continuous damage corridor	Consistent
Continuous narrow damage path	Generally absent	Not observed during field survey	Consistent
Convergent damage pattern	Generally absent	No convergent damage signatures identified	Consistent

Mesocyclone	Not associated with mesocyclonic rotation	No mesocyclone detected on DWR	Consistent
Tornado Vortex Signature (TVS)	Absent	No TVS identified	Consistent
Hook echo	Generally absent	No hook-like echo observed on radar reflectivity	Consistent
Persistent low-level rotation	Usually, absent	No persistent storm-scale rotation detected	Consistent

A comprehensive analysis of INSAT-3DR satellite imagery, Doppler Weather Radar (DWR) products collected from the C-band Doppler Weather Radar at Thiruvananthapuram (MAX (Z), PPI (Z), PPI(S), PPI (V), SRI, and HWV), synoptic weather charts, surface wind observations, eyewitness reports, and post-event damage survey findings indicates that the severe weather event over the Thoothukudi region on 21 June 2026 was associated with a localized severe convective thunderstorm. The radar products confirmed the presence of a mature convective cell exhibiting moderate to strong reflectivity and significant vertical development, capable of producing strong updrafts, downdrafts, damaging squally winds, and localized heavy rainfall. Surface observations at Thoothukudi Airport recorded a peak wind gust of approximately 28 knots, consistent with the passage of a thunderstorm gust front.

During the event, a funnel-like cloud accompanied by a rotating dust column was observed in the vicinity of Vagaikulam–Thoothukudi Airport. However, the available meteorological evidence does not satisfy the accepted diagnostic criteria for a tornado. Although the funnel-like cloud and dust column were evident, **there was no narrow continuous damage path, convergent damage pattern, persistent rotating damage track, Tornado Vortex Signature (TVS), hook echo, or persistent storm-scale mesocyclonic rotation in the Doppler Weather Radar observations.** Furthermore, the post-event field survey documented localized and discontinuous wind damage, which is inconsistent with the characteristic damage pattern produced by tornadoes.

To further evaluate the nature of the event, the observed meteorological and damage characteristics were systematically compared with the established diagnostic features of a gustnado (**Table 3**). As summarized in **Table 3**, all observed characteristics showed close agreement with the typical attributes of a gustnado. The event occurred in association with an intense convective thunderstorm and strong thunderstorm outflow, produced a localized rotating dust column and a funnel-like cloud beneath the cumulonimbus cloud, persisted only briefly, and caused localized, discontinuous damage confined to the Vagaikulam–Thoothukudi Airport sector. Moreover, the absence of a mesocyclone, Tornado Vortex Signature (TVS), hook echo, persistent low-level rotation, continuous narrow damage path, and convergent damage pattern further supports the interpretation that the vortex was non-mesocyclonic in nature.

Accordingly, based on the integrated analysis of satellite imagery, Doppler Weather Radar products, surface meteorological observations, eyewitness reports, post-event damage assessment, and the comparison presented in **Table 3, the event is best interpreted as a localized severe convective thunderstorm accompanied by a transient convective vortex or gustnado-like vortex, rather than a confirmed tornado**. This assessment is consistent with the available observational evidence and internationally accepted diagnostic criteria for distinguishing tornadoes from non-mesocyclonic convective vortices.

7. Operational Forecast Performance

The **Daily Weather Bulletin (DWB)** issued by the Regional Meteorological Centre (RMC), Chennai on **21 June 2026** indicated the likelihood of **light to moderate rain accompanied by thunderstorms and lightning at isolated places over southern districts of Tamil Nadu**, including **Thoothukudi district**, during the forecast period.

The prevailing synoptic conditions, including the favourable environment for convective development over southern Tamil Nadu, were reflected in the operational forecast. Subsequently, as convection intensified over the Thoothukudi region, radar-based nowcasting and aviation weather warnings were issued to provide location-specific short-range guidance.

Nowcast warnings

The convective weather situation over Tamil Nadu was continuously monitored using Doppler Weather Radar (DWR) observations and satellite imagery. Examination of the DWR image at **09:52:27 UTC (15:22 IST) on 21 June 2026** did not indicate any significant convective echo over the Thoothukudi district or its vicinity. Consequently, no nowcast warning was issued for Thoothukudi at that time, as the radar observations did not provide evidence of imminent convective development over the district.

Subsequent DWR observations at **11:31 UTC (17:01 IST)** showed the rapid development of a convective cell over the Thoothukudi district. Based on these radar observations, a **Nowcast Warning** was issued at **17:07 IST**, indicating **light to moderate rain accompanied by thunderstorm and lightning over isolated places in Thoothukudi, Tirunelveli, Tiruchirappalli, Virudhunagar, Cuddalore, and Puducherry during the next one to two hours**. The warning was disseminated through the operational nowcasting system and official communication channels, providing timely guidance regarding the developing convective weather.

The rapid initiation and intensification of the convective storm between the two radar scans highlights the highly dynamic nature of pre-monsoon convective systems over southern Tamil Nadu. The nowcast was issued promptly following the detection of significant convective echoes on Doppler Weather Radar, demonstrating the effectiveness of radar-based real-time monitoring for severe thunderstorm warning operations. This wording objectively explains why no earlier nowcast was issued while showing that IMD responded promptly once the radar detected the developing convective storm.

Thunderstorm/Gust Wind warnings

VOTK 211045Z AD WRNG 1 VALID 211105/211305 TSRA FCST NC=

METAR VOTK 211000Z 15006KT 5000 HZ SCT018 36/22 Q1006 NOSIG=
METAR VOTK 211030Z 15008KT 5000 HZ SCT018 35/22 Q1006 NOSIG=
METAR VOTK 211100Z 13010KT 5000 HZ SCT018 **FEW025CB** 35/23 Q1005 NOSIG=
METAR VOTK 211130Z 29010KT 4000 **TSRA** SCT018 **FEW025CB** 34/23 Q1007 NOSIG=
METAR VOTK 211200Z 14004KT 4000 **-TSRA** SCT018 **FEW025CB** 34/23 Q1007 TEMPO -TSRA=
METAR VOTK 211230Z VRB01KT 4000 HZ SCT018 **FEW025CB** 33/24 Q1007 NOSIG=

An **Aerodrome Warning (AD WRNG No. 1)** was issued for Thoothukudi Airport at **1045 UTC (1615 IST) on 21 June 2026**, valid from **1105 UTC to 1305 UTC (1635 IST to 1835 IST)**, forecasting **thunderstorm with rain (TSRA)** over the aerodrome. The warning period encompassed the occurrence of the severe convective weather event, including the funnel-like cloud feature observed near Thoothukudi Airport at approximately **1645–1700 IST**. This indicates that the operational aviation weather forecasting system had anticipated thunderstorm activity affecting the airport during the period of the event.

Airport Terminal Aerodrome Forecast (TAF)

TAF VOTK 210200Z 2103/2112 23005KT 5000 HZ FEW018 BECMG 2108/2109 14010KT=
TAF VOTK 210500Z 2106/2115 29010KT 6000 FEW020 SCT100 BECMG 2109/2110 14010KT=
TAF VOTK 210800Z 2109/2118 14010KT 6000 FEW020 SCT100=

The Terminal Aerodrome Forecasts (TAFs) issued for Thoothukudi Airport (VOTK) during 21 June 2026 forecast prevailing fair-weather conditions with scattered low and middle clouds and gradual changes in surface wind direction. None of the routine TAFs explicitly indicated the occurrence of thunderstorms, cumulonimbus (CB) clouds, or gusty winds, as no significant convective development was evident at the respective times of issuance. The rapid initiation and intensification of the convective storm occurred after the issuance of the routine TAFs and was subsequently captured through Doppler Weather Radar observations, enabling the timely issuance of an Aerodrome Warning and a radar-based nowcast.

The **Daily Weather Bulletin** issued by RMC Chennai on **21 June 2026** indicated the likelihood of light to moderate rain with thunderstorms and lightning over isolated places in southern Tamil Nadu, including **Thoothukudi district**. The routine **Terminal Aerodrome Forecasts (TAFs)** issued at **0200 UTC, 0500 UTC, and 0800 UTC** did not explicitly forecast thunderstorms or gusty winds, as no significant convective development was evident at the time of issuance.

The **09:52 UTC Doppler Weather Radar** scan did not show significant convective echoes over Thoothukudi; therefore, no nowcast warning was issued at that stage. However, the **11:00 UTC radar** scan detected rapid development of a convective cell over the district, following which a **Nowcast Warning** was issued at **1707 IST** for thunderstorms and lightning over Thoothukudi and adjoining districts. Additionally, an **Aerodrome Warning**

(VOTK AD WRNG No. 1) was issued at **1045 UTC (1615 IST)**, valid from **1105 UTC to 1305 UTC**, forecasting **thunderstorm with rain (TSRA)** over Thoothukudi Airport.

Overall, the operational forecasting system successfully anticipated the potential for convective weather through the Daily Weather Bulletin, while real-time Doppler Weather Radar monitoring enabled the timely issuance of nowcast and aviation warnings as the thunderstorm rapidly developed over the Thoothukudi region

8. Final Conclusion

Based on a comprehensive analysis of **synoptic weather conditions, INSAT-3DR satellite imagery, Doppler Weather Radar (DWR) products from the IMD C-band Doppler Weather Radar at Thiruvananthapuram, surface meteorological observations, airport wind records, eyewitness accounts, photographic and video evidence, and post-event field damage surveys**, the severe weather event that affected parts of **Thoothukudi district on 21 June 2026** is assessed to have been a **localized severe convective thunderstorm** embedded within the southwest monsoon environment.

The thunderstorm developed under the influence of an **east–west trough at the 700 hPa level**, which, together with enhanced low-level moisture convergence, atmospheric instability, and daytime heating, favoured the rapid development of a mature cumulonimbus cloud. The storm produced strong convective updrafts and downdrafts, damaging squally winds, localized heavy rainfall, lightning, and transient rotational features.

A **funnel-like cloud** accompanied by a **rotating dust column** was observed near the **Vagaikulam–Thoothukudi Airport** area during the peak stage of the thunderstorm. Surface observations recorded a peak wind gust of approximately **28 knots**, while post-event damage assessment indicates that localized wind speeds in the most severely affected areas were considerably higher, with estimated peak gusts possibly exceeding **60 knots (≈110 km h^{-1})**. The observed damage, including roof failures, uprooted trees, scattered debris, and damage to light structures and utility infrastructure, is consistent with severe convective wind phenomena associated with localized downbursts and thunderstorm outflow.

Detailed comparison of the observed meteorological conditions with established tornado and gustnado diagnostic criteria indicates that the event **does not satisfy the requirements for classification as a tornado**. The field investigation did not identify a continuous narrow damage path or convergent damage pattern, while Doppler Weather Radar observations showed **no Tornado Vortex Signature (TVS), hook echo, mesocyclone, or persistent storm-scale rotation**. These findings are inconsistent with a tornadic circulation.

Conversely, the observed characteristics—including the occurrence during an intense convective thunderstorm, strong gust-front outflow, localized rotating dust column beneath the cumulonimbus cloud, short duration, highly localized and discontinuous damage pattern, and the absence of mesocyclonic rotation—closely match the documented characteristics of a **gustnado**, a shallow, non-mesocyclonic vortex that develops along the gust front of severe thunderstorms.

Accordingly, the severe weather event over Thoothukudi on 21 June 2026 is best interpreted as a localized severe convective thunderstorm producing damaging squally winds, localized microburst/downburst effects, and a transient gustnado-like convective vortex, rather than a confirmed tornado. While a funnel-like cloud and localized rotation were observed, the available meteorological, radar, and damage evidence is insufficient to support classification of the event as a tornado.

The event demonstrates that severe convective storms embedded within the southwest monsoon can produce highly localized but damaging wind phenomena over southern Tamil Nadu. It also highlights the importance of integrating **satellite observations, Doppler Weather Radar velocity products, surface meteorological observations, and systematic post-event damage surveys** for accurate diagnosis of localized severe weather events and for improving future warning services and disaster preparedness.

Attachments:

1. **Annexure-I.**
2. Photographs/Videos

Annexure-I.

PHOTOGRAPHIC EVIDENCE: LOSS OF ROOF TILES IN RESIDENTIAL BUILDINGS AT MUDIVAITHANENDAL: **Photo Source: IMD official**

Photo Source: IMD official

Photo Source: IMD official

PHOTOGRAPHIC EVIDENCE: VAGAIKULAM THEME PARK

Photo Source: IMD official

Damage to a private amusement/theme park

PHOTOGRAPHIC EVIDENCE: VAGAIKULAM TOLL PLAZA

Photo Source: IMD official

DWR OBSERVATIONS; Maximum Reflectivity (MAX(Z))

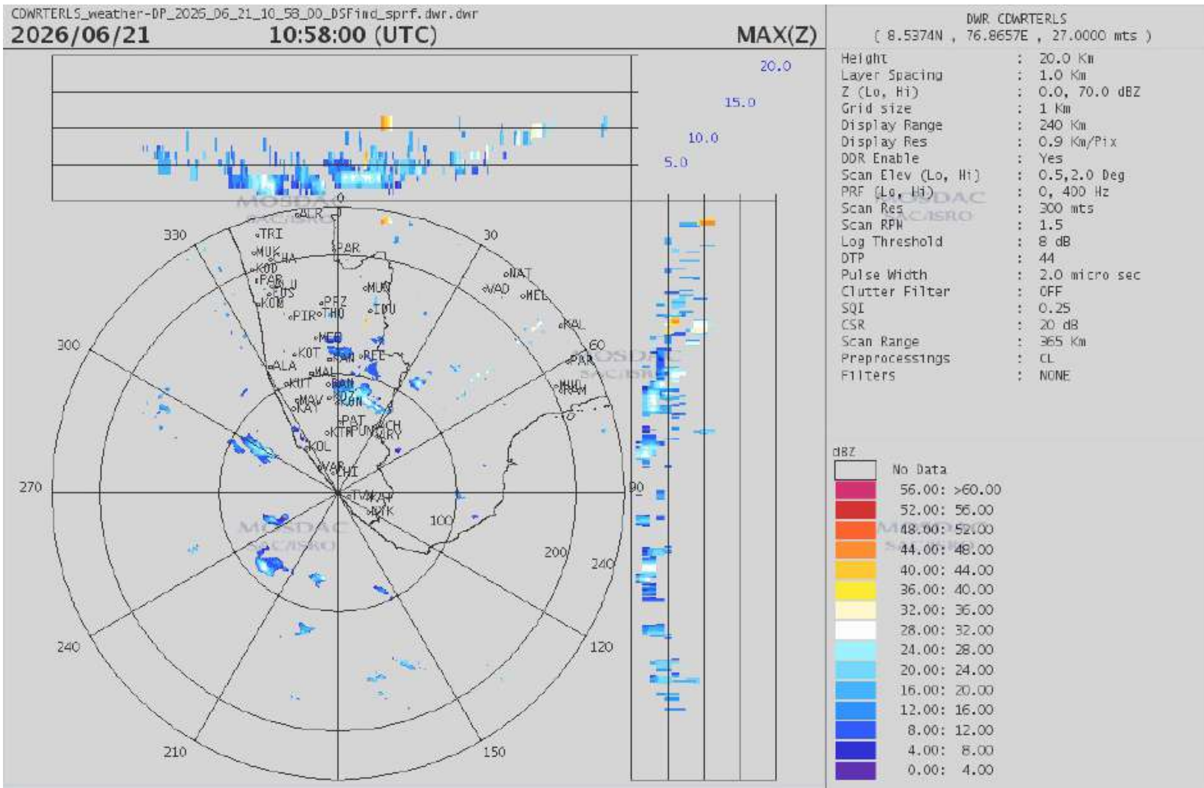

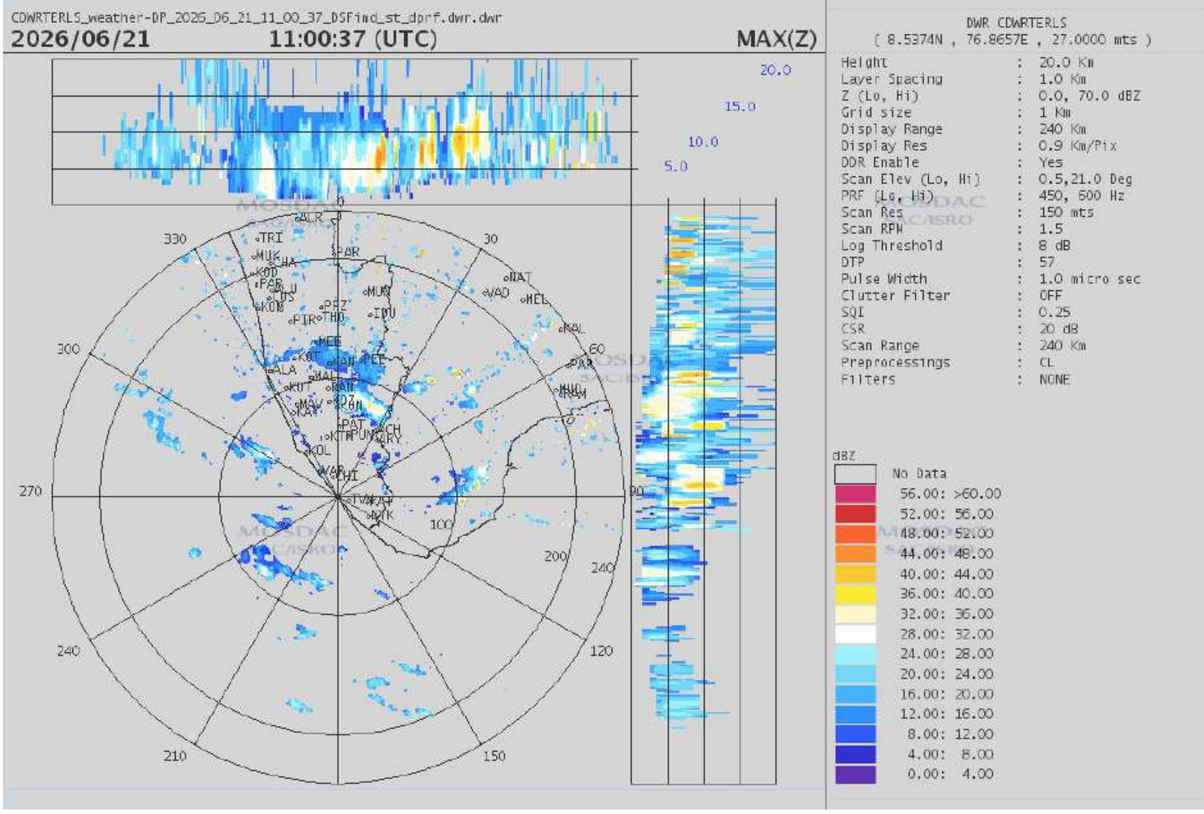

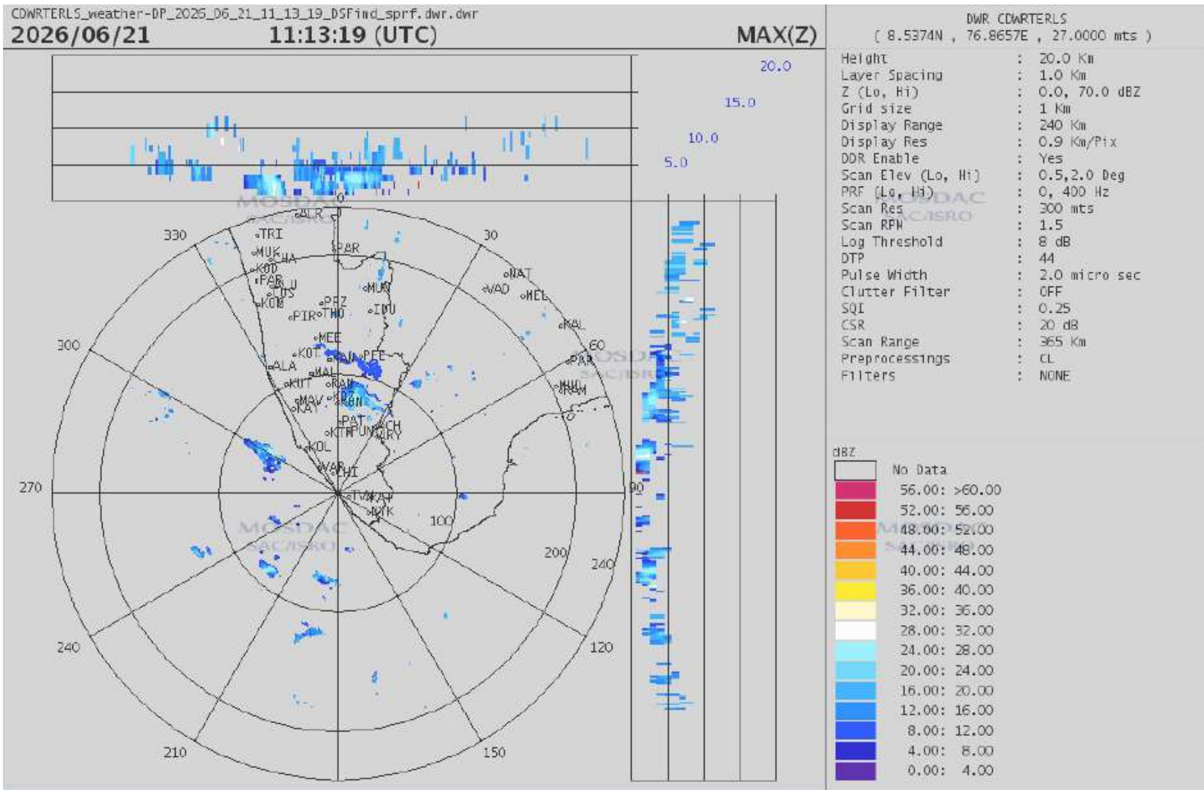
CDWRTERLS_weather-DP_2026_06_21_11_13_19_DSFind_sprf.dwr.dwr
2026/06/21
11:13:19 (UTC)
MAX(Z)
DWR CDWRTERLS
(8.5374N , 76.8657E , 27.0000 mts)
Height : 20.0 Km
Layer Spacing : 1.0 Km
Z (Lo, Hi) : 0.0, 70.0 dBZ
Grid size : 1 Km
Display Range : 240 Km
Display Res : 0.9 Km/Pix
DDR Enable : Yes
Scan Elev (Lo, Hi) : 0.5,2.0 Deg
PRF (Lo, Hi) : 0, 400 Hz
Scan Res : 300 mts
Scan RPM : 1.5
Log Threshold : 8 dB
DTP : 44
Pulse Width : 2.0 micro sec
Clutter Filter : OFF
SQI : 0.25
CSR : 20 dB
Scan Range : 365 Km
Preprocessings : CL
Filters : NONE
dBZ
No Data
56.00: >60.00
52.00: 56.00
48.00: 52.00
44.00: 48.00
40.00: 44.00
36.00: 40.00
32.00: 36.00
28.00: 32.00
24.00: 28.00
20.00: 24.00
16.00: 20.00
12.00: 16.00
8.00: 12.00
4.00: 8.00
0.00: 4.00

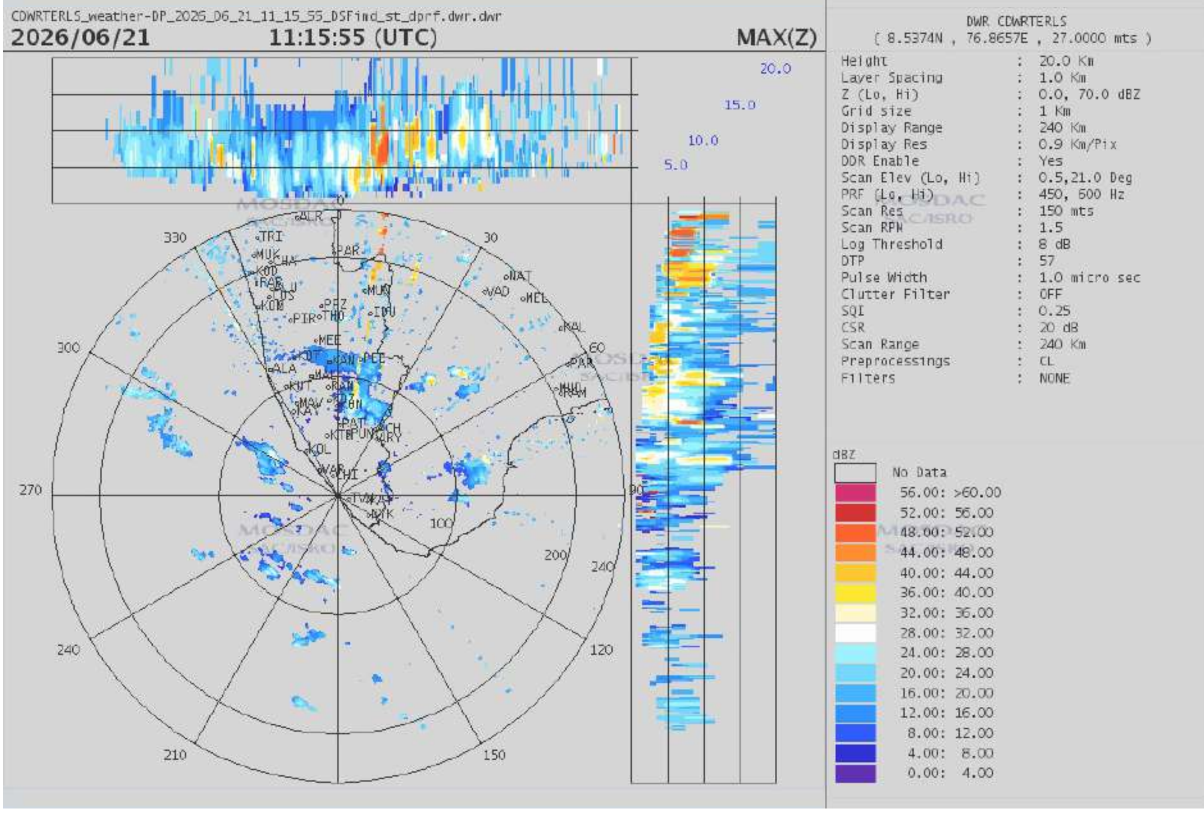
CDWRTERLS_weather-DP_2026_06_21_11_15_55_DSFind_st_dprf.dwr.dwr
2026/06/21
11:15:55 (UTC)
MAX(Z)
DWR CDWRTERLS
(8.5374N , 76.8657E , 27.0000 mts)
Height : 20.0 Km
Layer Spacing : 1.0 Km
Z (Lo, Hi) : 0.0, 70.0 dBZ
Grid size : 1 Km
Display Range : 240 Km
Display Res : 0.9 Km/Pix
DDR Enable : Yes
Scan Elev (Lo, Hi) : 0.5,21.0 Deg
PRF (Lo, Hi) : 450, 600 Hz
Scan Res : 150 mts
Scan RPM : 1.5
Log Threshold : 8 dB
DTP : 57
Pulse Width : 1.0 micro sec
Clutter Filter : OFF
SQI : 0.25
CSR : 20 dB
Scan Range : 240 Km
Preprocessings : CL
Filters : NONE
dBZ
No Data
56.00: >60.00
52.00: 56.00
48.00: 52.00
44.00: 48.00
40.00: 44.00
36.00: 40.00
32.00: 36.00
28.00: 32.00
24.00: 28.00
20.00: 24.00
16.00: 20.00
12.00: 16.00
8.00: 12.00
4.00: 8.00
0.00: 4.00

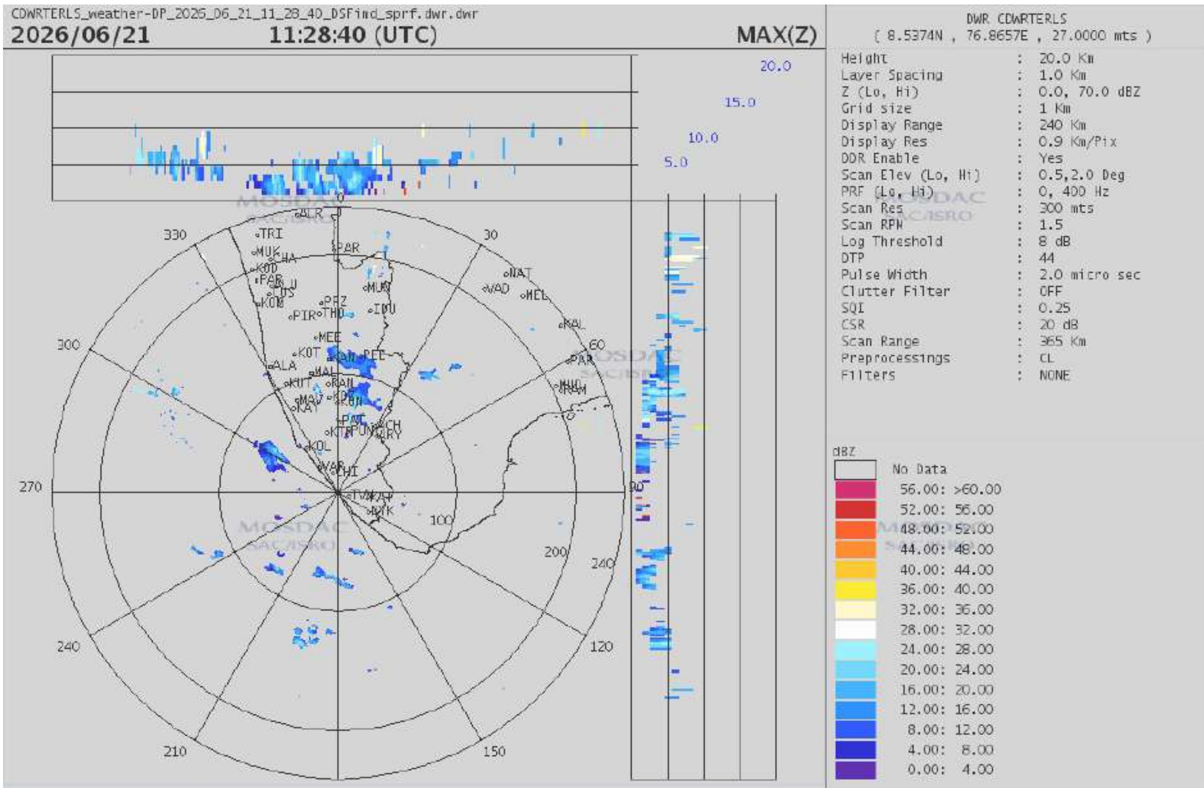
CDWRTERLS_weather-DP_2026_06_21_11_28_40_DSFind_sprf.dwr.dwr
2026/06/21
11:28:40 (UTC)
MAX(Z)
DWR CDWRTERLS
(8.5374N , 76.8657E , 27.0000 mts)
Height : 20.0 Km
Layer Spacing : 1.0 Km
Z (Lo, Hi) : 0.0, 70.0 dBZ
Grid size : 1 Km
Display Range : 240 Km
Display Res : 0.9 Km/Pix
DDR Enable : Yes
Scan Elev (Lo, Hi) : 0.5,2.0 Deg
PRF (Lo, Hi) : 0, 400 Hz
Scan Res : 300 mts
Scan RPM : 1.5
Log Threshold : 8 dB
DTP : 44
Pulse Width : 2.0 micro sec
Clutter Filter : OFF
SQI : 0.25
CSR : 20 dB
Scan Range : 365 Km
Preprocessings : CL
Filters : NONE
dBZ
No Data
56.00: >60.00
52.00: 56.00
48.00: 52.00
44.00: 48.00
40.00: 44.00
36.00: 40.00
32.00: 36.00
28.00: 32.00
24.00: 28.00
20.00: 24.00
16.00: 20.00
12.00: 16.00
8.00: 12.00
4.00: 8.00
0.00: 4.00

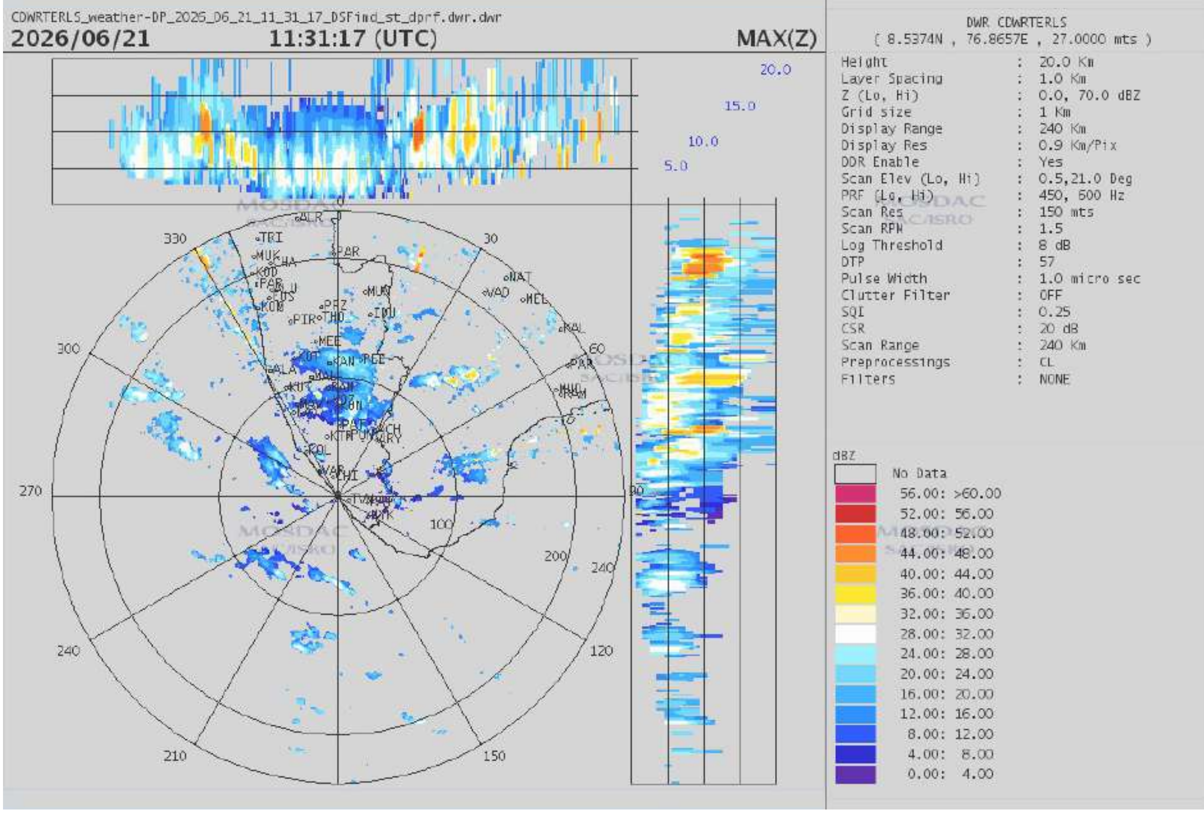
CDWRTERLS_weather-DP_2026_06_21_11_31_17_DSFind_st_dprf.dwr.dwr
2026/06/21
11:31:17 (UTC)
MAX(Z)
DWR CDWRTERLS
(8.5374N , 76.8657E , 27.0000 mts)
Height : 20.0 Km
Layer Spacing : 1.0 Km
Z (Lo, Hi) : 0.0, 70.0 dBZ
Grid size : 1 Km
Display Range : 240 Km
Display Res : 0.9 Km/Pix
DDR Enable : Yes
Scan Elev (Lo, Hi) : 0.5,21.0 Deg
PRF (Lo, Hi) : 450, 600 Hz
Scan Res : 150 mts
Scan RPM : 1.5
Log Threshold : 8 dB
DTP : 57
Pulse Width : 1.0 micro sec
Clutter Filter : OFF
SQI : 0.25
CSR : 20 dB
Scan Range : 240 Km
Preprocessings : CL
Filters : NONE
dBZ
No Data
56.00: >60.00
52.00: 56.00
48.00: 52.00
44.00: 48.00
40.00: 44.00
36.00: 40.00
32.00: 36.00
28.00: 32.00
24.00: 28.00
20.00: 24.00
16.00: 20.00
12.00: 16.00
8.00: 12.00
4.00: 8.00
0.00: 4.00

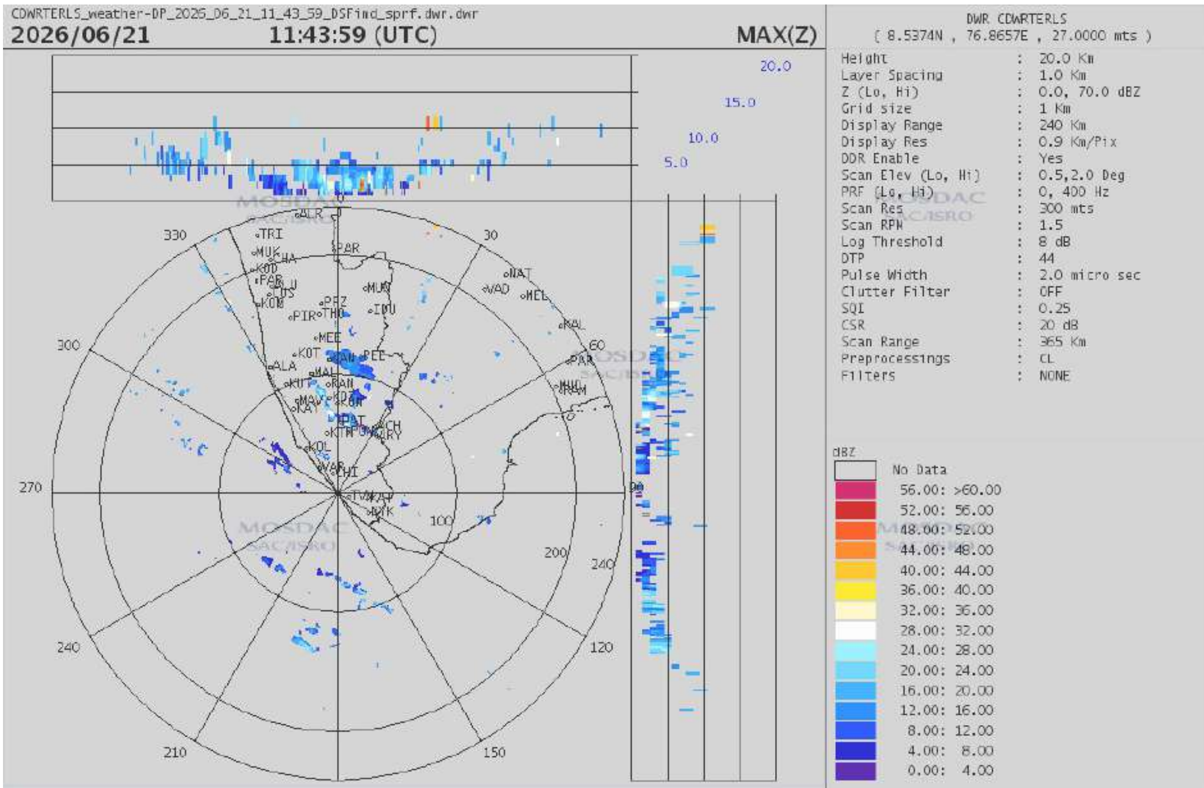
CDWRTERLS_weather-DP_2026_06_21_11_43_59_DSFind_sprf.dwr.dwr
2026/06/21
11:43:59 (UTC)
MAX(Z)
DWR CDWRTERLS
(8.5374N , 76.8657E , 27.0000 mts)
Height : 20.0 Km
Layer Spacing : 1.0 Km
Z (Lo, Hi) : 0.0, 70.0 dBZ
Grid size : 1 Km
Display Range : 240 Km
Display Res : 0.9 Km/Pix
DDR Enable : Yes
Scan Elev (Lo, Hi) : 0.5,2.0 Deg
PRF (Lo, Hi) : 0, 400 Hz
Scan Res : 300 mts
Scan RPM : 1.5
Log Threshold : 8 dB
DTP : 44
Pulse Width : 2.0 micro sec
Clutter Filter : OFF
SQI : 0.25
CSR : 20 dB
Scan Range : 365 Km
Preprocessings : CL
Filters : NONE
dBZ
No Data
56.00: >60.00
52.00: 56.00
48.00: 52.00
44.00: 48.00
40.00: 44.00
36.00: 40.00
32.00: 36.00
28.00: 32.00
24.00: 28.00
20.00: 24.00
16.00: 20.00
12.00: 16.00
8.00: 12.00
4.00: 8.00
0.00: 4.00

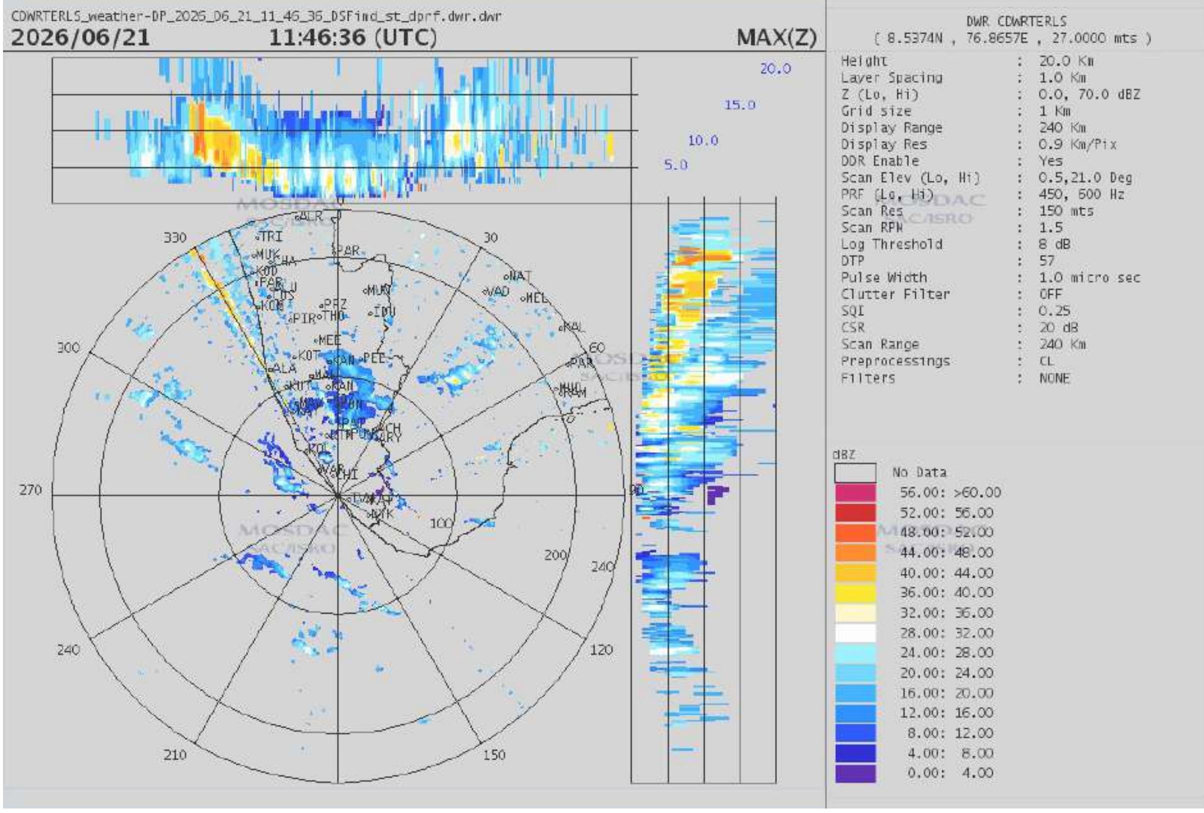
CDWRTERLS_weather-DP_2026_06_21_11_46_36_DSFind_st_dprf.dwr.dwr
2026/06/21
11:46:36 (UTC)
MAX(Z)
DWR CDWRTERLS
(8.5374N , 76.8657E , 27.0000 mts)
Height : 20.0 Km
Layer Spacing : 1.0 Km
Z (Lo, Hi) : 0.0, 70.0 dBZ
Grid size : 1 Km
Display Range : 240 Km
Display Res : 0.9 Km/Pix
DDR Enable : Yes
Scan Elev (Lo, Hi) : 0.5,21.0 Deg
PRF (Lo, Hi) : 450, 600 Hz
Scan Res : 150 mts
Scan RPM : 1.5
Log Threshold : 8 dB
DTP : 57
Pulse Width : 1.0 micro sec
Clutter Filter : OFF
SQI : 0.25
CSR : 20 dB
Scan Range : 240 Km
Preprocessings : CL
Filters : NONE
dBZ
No Data
56.00: >60.00
52.00: 56.00
48.00: 52.00
44.00: 48.00
40.00: 44.00
36.00: 40.00
32.00: 36.00
28.00: 32.00
24.00: 28.00
20.00: 24.00
16.00: 20.00
12.00: 16.00
8.00: 12.00
4.00: 8.00
0.00: 4.00

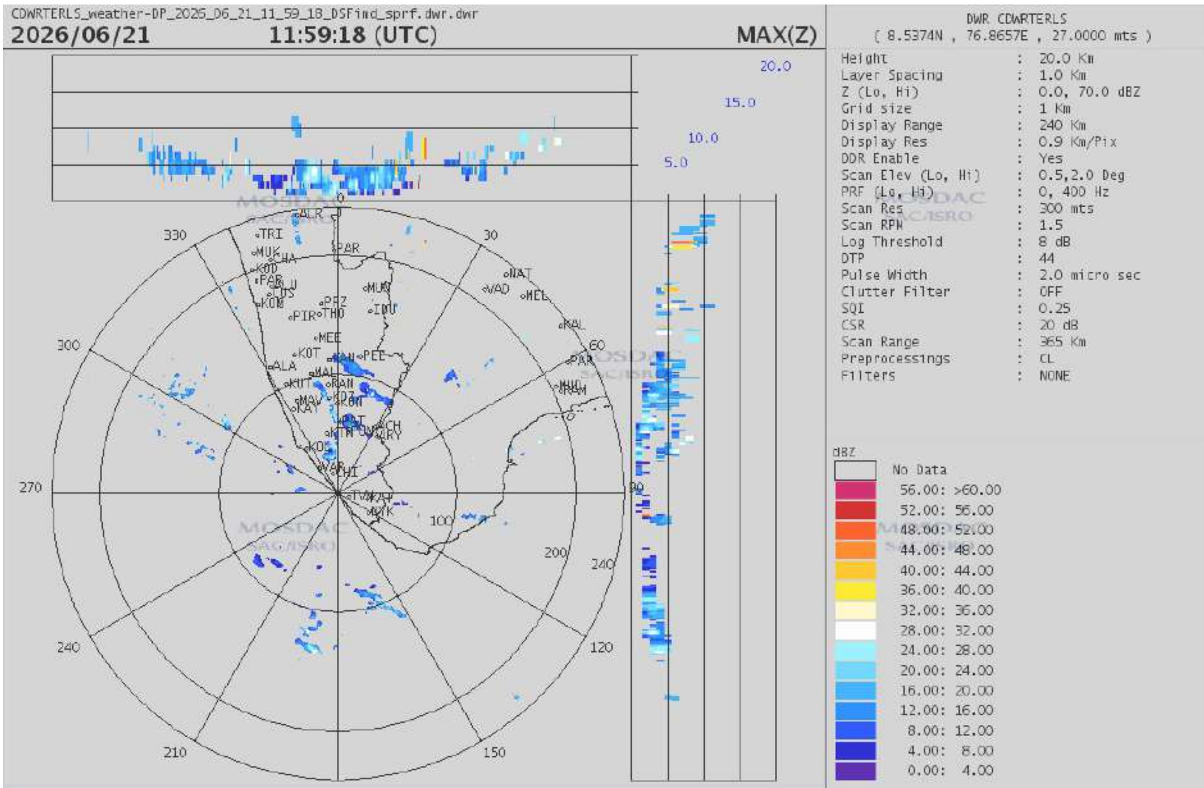
CDWRTERLS_weather-DP_2026_06_21_11_59_18_DSFind_sprf.dwr.dwr
2026/06/21
11:59:18 (UTC)
MAX(Z)
DWR CDWRTERLS
(8.5374N , 76.8657E , 27.0000 mts)
Height : 20.0 Km
Layer Spacing : 1.0 Km
Z (Lo, Hi) : 0.0, 70.0 dBZ
Grid size : 1 Km
Display Range : 240 Km
Display Res : 0.9 Km/Pix
DDR Enable : Yes
Scan Elev (Lo, Hi) : 0.5,2.0 Deg
PRF (Lo, Hi) : 0, 400 Hz
Scan Res : 300 mts
Scan RPM : 1.5
Log Threshold : 8 dB
DTP : 44
Pulse Width : 2.0 micro sec
Clutter Filter : OFF
SQI : 0.25
CSR : 20 dB
Scan Range : 365 Km
Preprocessings : CL
Filters : NONE
dBZ
No Data
56.00: >60.00
52.00: 56.00
48.00: 52.00
44.00: 48.00
40.00: 44.00
36.00: 40.00
32.00: 36.00
28.00: 32.00
24.00: 28.00
20.00: 24.00
16.00: 20.00
12.00: 16.00
8.00: 12.00
4.00: 8.00
0.00: 4.00

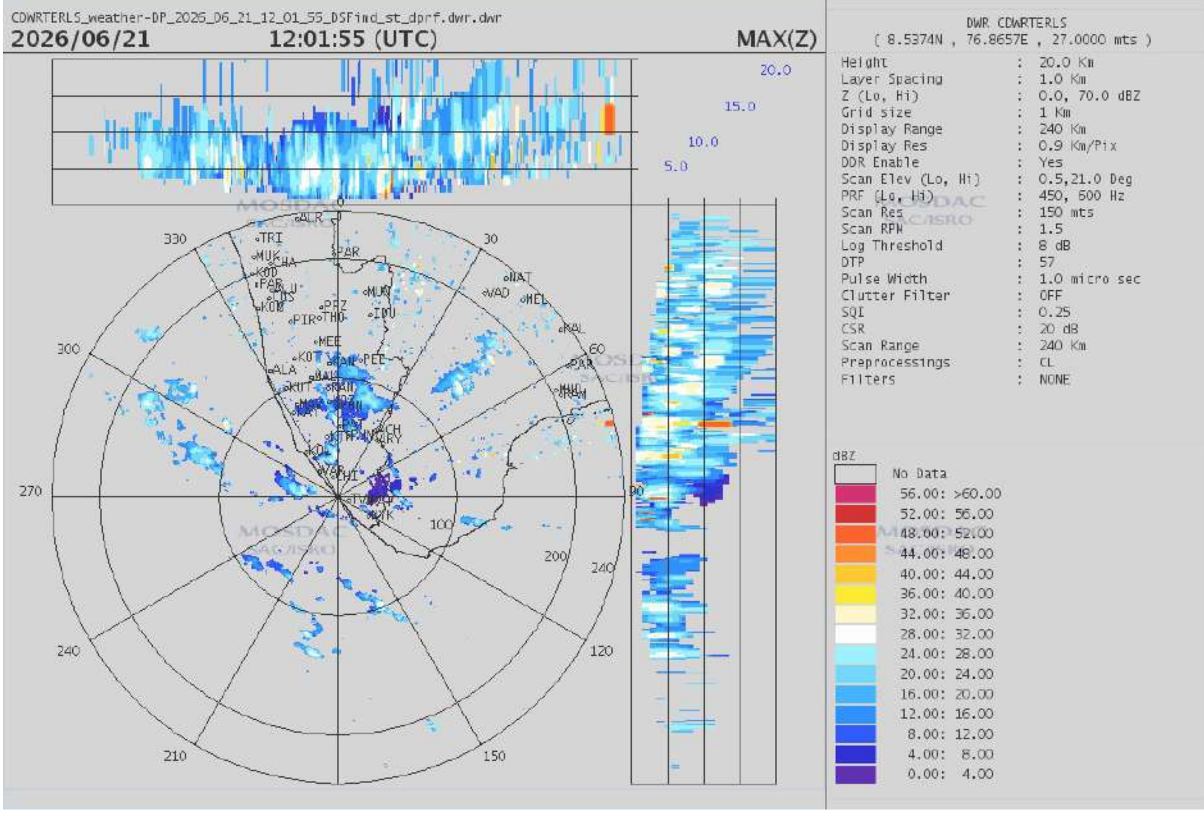
CDWRTERLS_weather-DP_2026_06_21_12_01_55_DSFind_st_dprf.dwr.dwr
2026/06/21
12:01:55 (UTC)
MAX(Z)
DWR CDWRTERLS
(8.5374N , 76.8657E , 27.0000 mts)
Height : 20.0 Km
Layer Spacing : 1.0 Km
Z (Lo, Hi) : 0.0, 70.0 dBZ
Grid size : 1 Km
Display Range : 240 Km
Display Res : 0.9 Km/Pix
DDR Enable : Yes
Scan Elev (Lo, Hi) : 0.5,21.0 Deg
PRF (Lo, Hi) : 450, 600 Hz
Scan Res : 150 mts
Scan RPM : 1.5
Log Threshold : 8 dB
DTP : 57
Pulse Width : 1.0 micro sec
Clutter Filter : OFF
SQI : 0.25
CSR : 20 dB
Scan Range : 240 Km
Preprocessings : CL
Filters : NONE
dBZ
No Data
56.00: >60.00
52.00: 56.00
48.00: 52.00
44.00: 48.00
40.00: 44.00
36.00: 40.00
32.00: 36.00
28.00: 32.00
24.00: 28.00
20.00: 24.00
16.00: 20.00
12.00: 16.00
8.00: 12.00
4.00: 8.00
0.00: 4.00

DWR OBSERVATIONS; PPI(V) - Plan Position Indicator Velocity

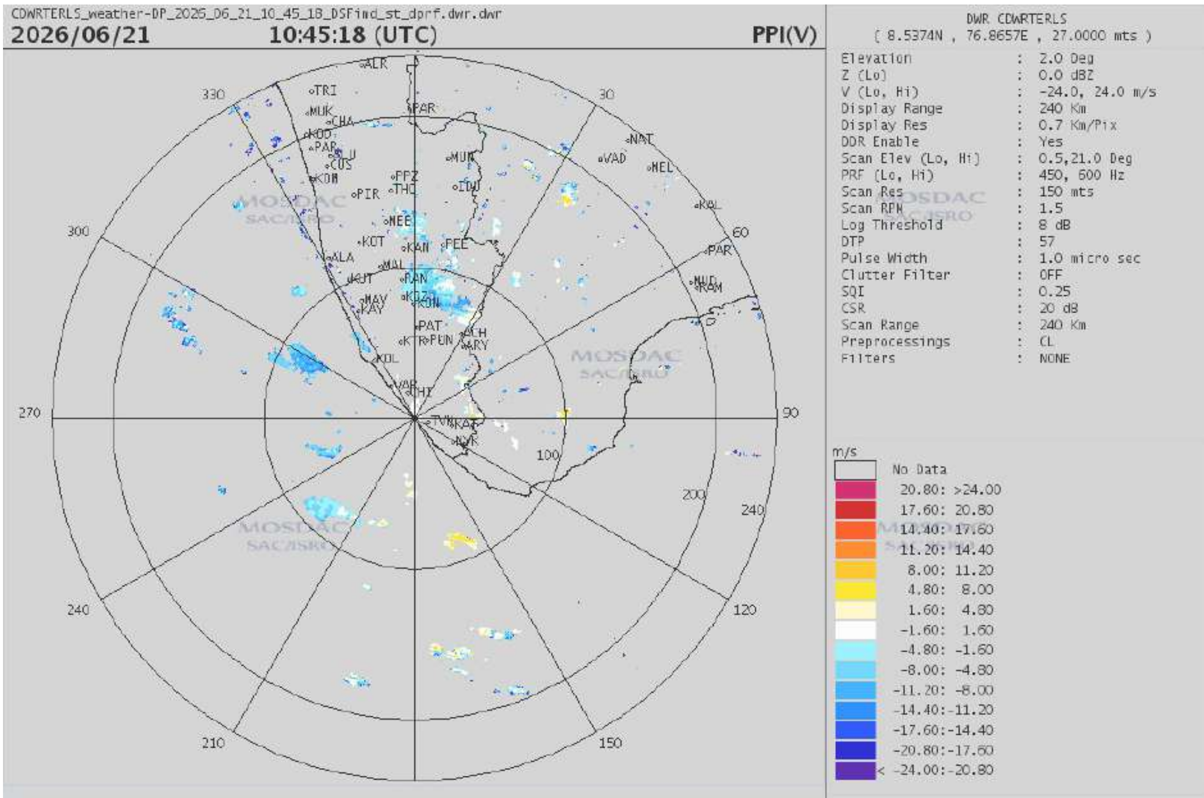

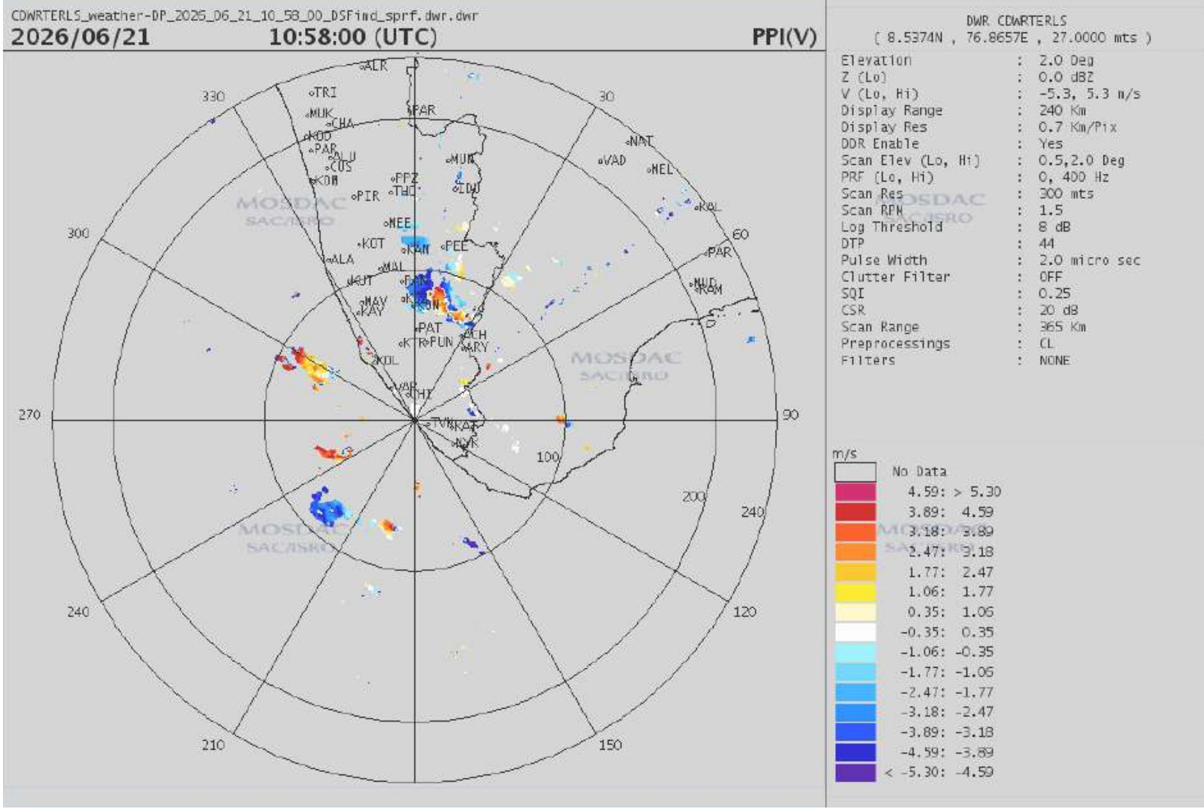

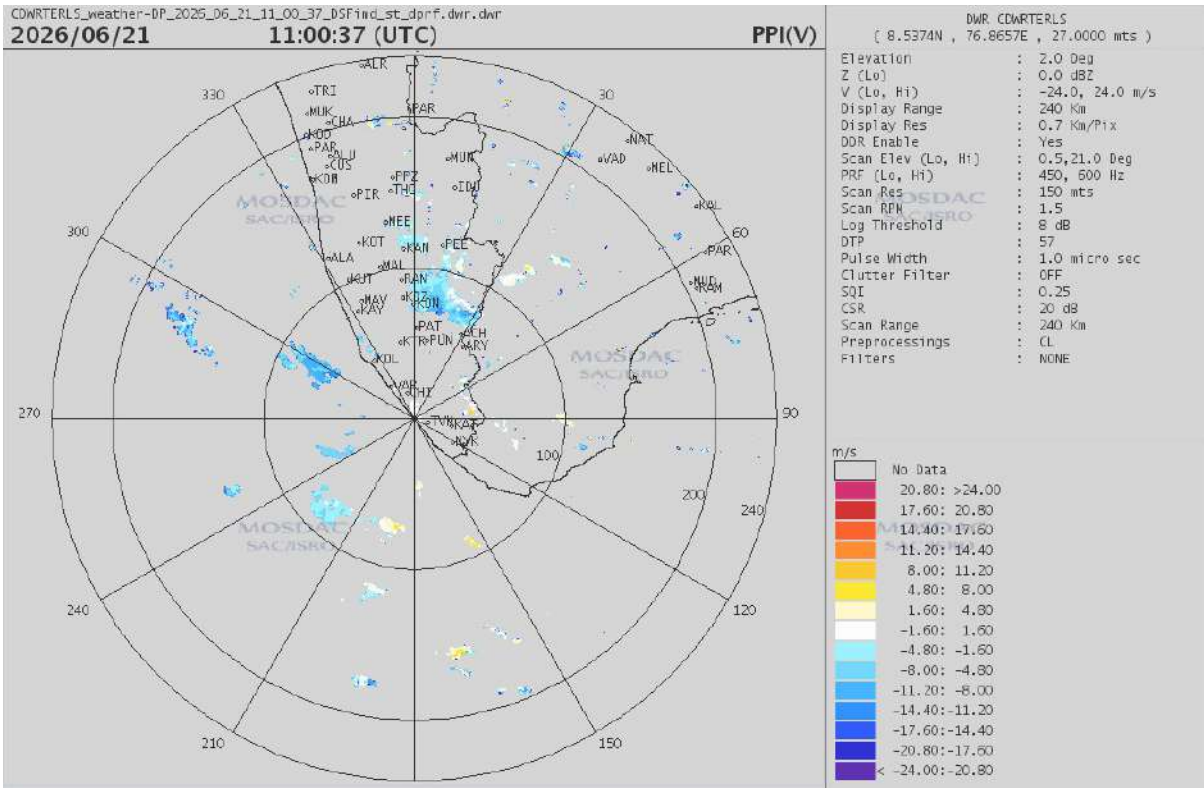
CDWRTERLS_weather-DP_2025_06_21_11_00_37_DSFind_st_dprf.dwr.dwr
2026/06/21
11:00:37 (UTC)
PPI(V)
DWR CDWRTERLS
(8.5374N , 76.8657E , 27.0000 mts)
Elevation : 2.0 Deg
Z (Lo) : 0.0 dBZ
V (Lo, Hi) : -24.0, 24.0 m/s
Display Range : 240 Km
Display Res : 0.7 Km/Pix
DDR Enable : Yes
Scan Elev (Lo, Hi) : 0.5,21.0 Deg
PRF (Lo, Hi) : 450, 600 Hz
Scan Res : 150 mts
Scan RPM : 1.5
Log Threshold : 8 dB
DTP : 57
Pulse Width : 1.0 micro sec
Clutter Filter : OFF
SQI : 0.25
CSR : 20 dB
Scan Range : 240 Km
Preprocessings : CL
Filters : NONE
m/s
No Data
20.80: >24.00
17.60: 20.80
14.40: 17.60
11.20: 14.40
8.00: 11.20
4.80: 8.00
1.60: 4.80
-1.60: 1.60
-4.80: -1.60
-8.00: -4.80
-11.20: -8.00
-14.40: -11.20
-17.60: -14.40
-20.80: -17.60
< -24.00: -20.80

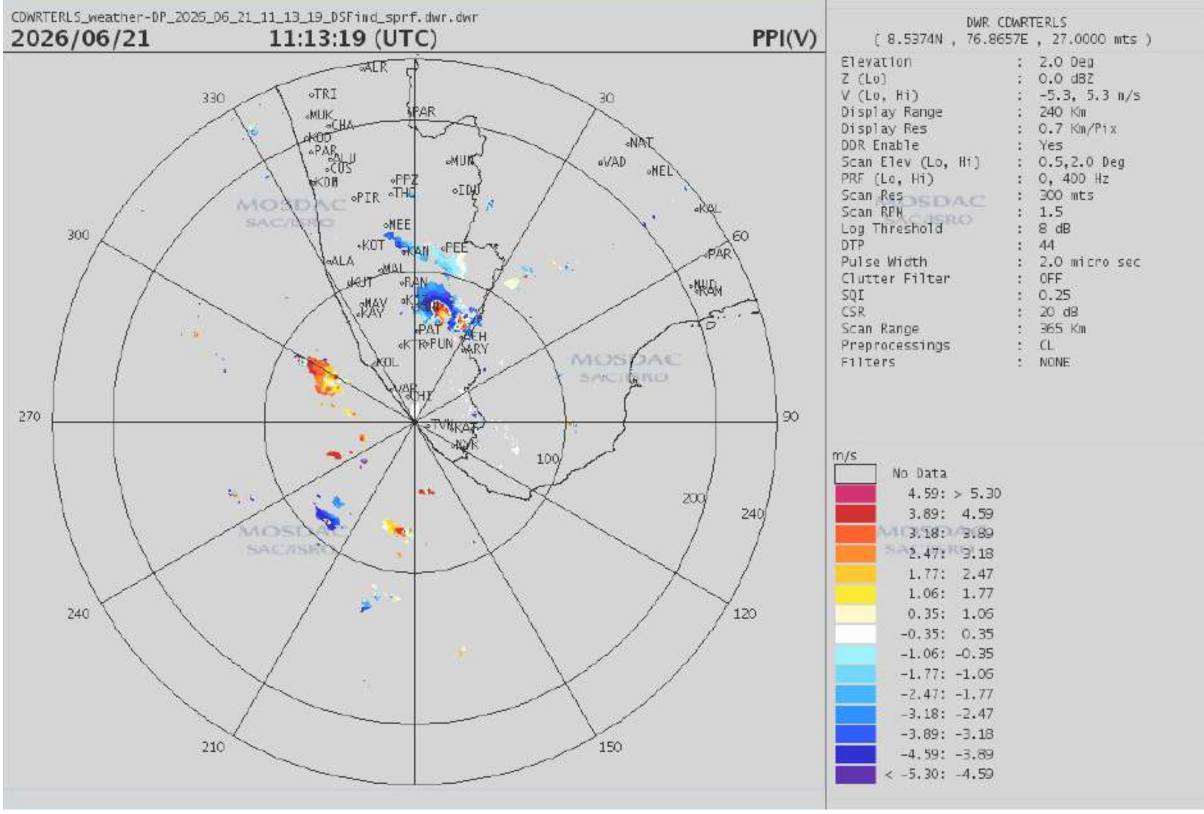
CDWRTERLS_weather-DP_2025_06_21_11_13_19_DSFind_sprf.dwr.dwr
2026/06/21
11:13:19 (UTC)
PPI(V)
DWR CDWRTERLS
(8.5374N , 76.8657E , 27.0000 mts)
Elevation : 2.0 Deg
Z (Lo) : 0.0 dBZ
V (Lo, Hi) : -5.3, 5.3 m/s
Display Range : 240 Km
Display Res : 0.7 Km/Pix
DDR Enable : Yes
Scan Elev (Lo, Hi) : 0.5,2.0 Deg
PRF (Lo, Hi) : 0, 400 Hz
Scan Res : 300 mts
Scan RPM : 1.5
Log Threshold : 8 dB
DTP : 44
Pulse Width : 2.0 micro sec
Clutter Filter : OFF
SQI : 0.25
CSR : 20 dB
Scan Range : 365 Km
Preprocessings : CL
Filters : NONE
m/s
No Data
4.59: > 5.30
3.89: 4.59
3.18: 3.89
2.47: 3.18
1.77: 2.47
1.06: 1.77
0.35: 1.06
-0.35: 0.35
-1.06: -0.35
-1.77: -1.06
-2.47: -1.77
-3.18: -2.47
-3.89: -3.18
-4.59: -3.89
< -5.30: -4.59

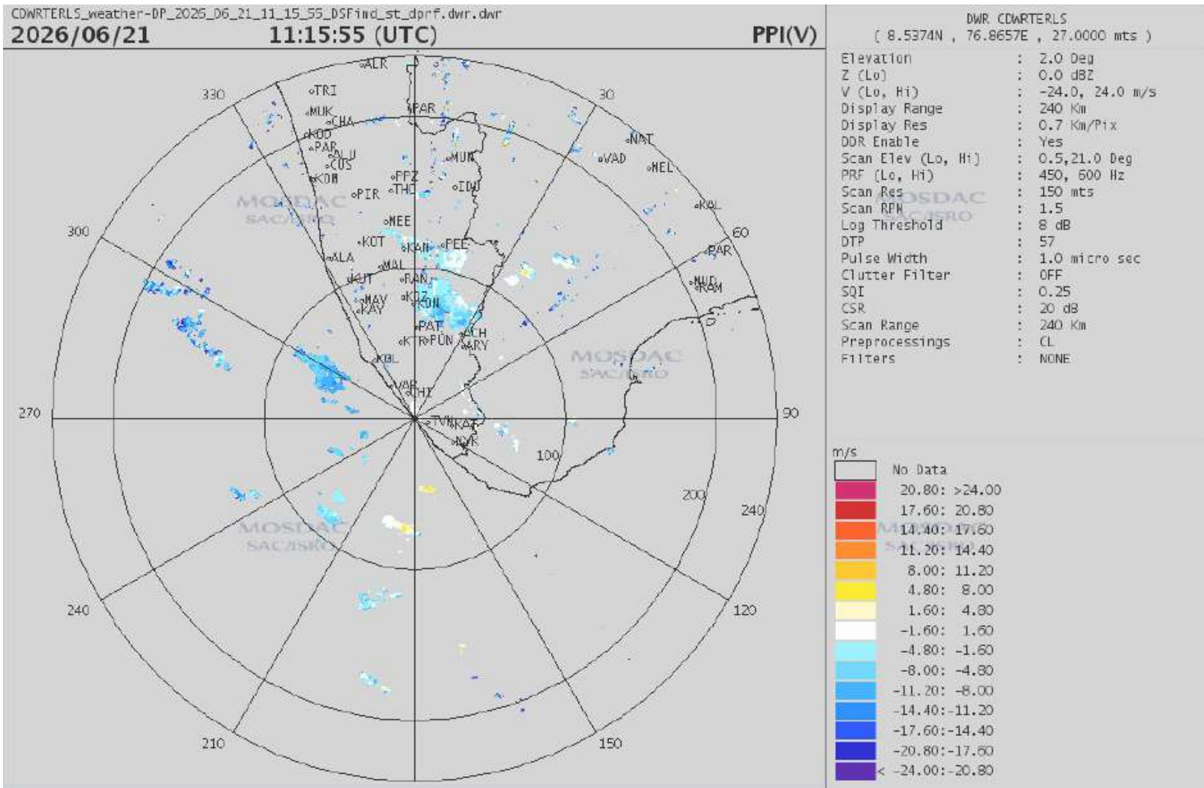

CDWRTERLS_weather-DP_2026_06_21_11_15_55_DSFind_st_dprf.dwr.dwr
2026/06/21
11:15:55 (UTC)
PPI(V)
DWR CDWRTERLS
(8.5374N , 76.8657E , 27.0000 mts)
Elevation : 2.0 Deg
Z (Lo) : 0.0 dBZ
V (Lo, Hi) : -24.0, 24.0 m/s
Display Range : 240 Km
Display Res : 0.7 Km/Pix
DDR Enable : Yes
Scan Elev (Lo, Hi) : 0.5,21.0 Deg
PRF (Lo, Hi) : 450, 600 Hz
Scan Res : 150 mts
Scan RPM : 1.5
Log Threshold : 8 dB
DTP : 57
Pulse Width : 1.0 micro sec
Clutter Filter : OFF
SQI : 0.25
CSR : 20 dB
Scan Range : 240 Km
Preprocessings : CL
Filters : NONE
m/s
No Data
20.80: >24.00
17.60: 20.80
14.40: 17.60
11.20: 14.40
8.00: 11.20
4.80: 8.00
1.60: 4.80
-1.60: 1.60
-4.80: -1.60
-8.00: -4.80
-11.20: -8.00
-14.40: -11.20
-17.60: -14.40
-20.80: -17.60
< -24.00: -20.80

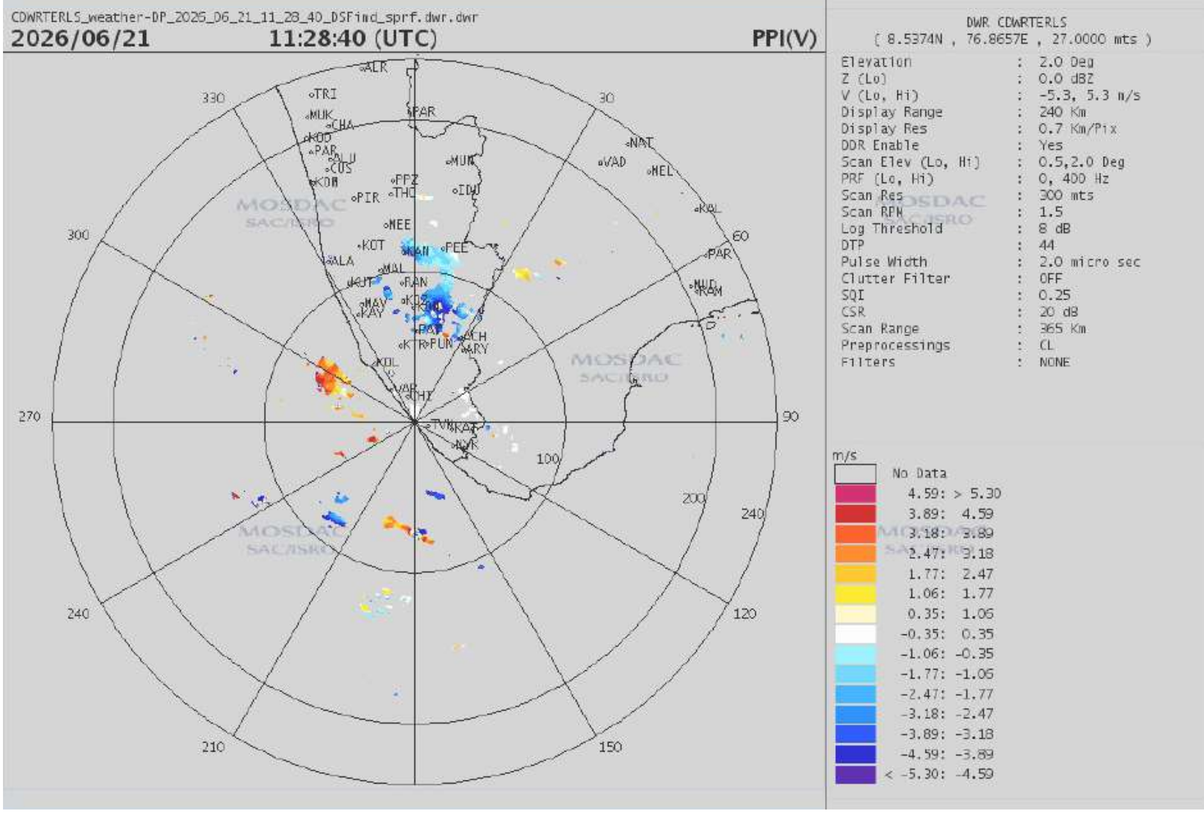

CDWRTERLS_weather-DP_2026_06_21_11_28_40_DSFind_sprf.dwr.dwr
2026/06/21
11:28:40 (UTC)
PPI(V)
DWR CDWRTERLS
(8.5374N , 76.8657E , 27.0000 mts)
Elevation : 2.0 Deg
Z (Lo) : 0.0 dBZ
V (Lo, Hi) : -5.3, 5.3 m/s
Display Range : 240 Km
Display Res : 0.7 Km/Pix
DDR Enable : Yes
Scan Elev (Lo, Hi) : 0.5,2.0 Deg
PRF (Lo, Hi) : 0, 400 Hz
Scan Res : 300 mts
Scan RPM : 1.5
Log Threshold : 8 dB
DTP : 44
Pulse Width : 2.0 micro sec
Clutter Filter : OFF
SQI : 0.25
CSR : 20 dB
Scan Range : 365 Km
Preprocessings : CL
Filters : NONE
m/s
No Data
4.59: > 5.30
3.89: 4.59
3.18: 3.89
2.47: 3.18
1.77: 2.47
1.06: 1.77
0.35: 1.06
-0.35: 0.35
-1.06: -0.35
-1.77: -1.06
-2.47: -1.77
-3.18: -2.47
-3.89: -3.18
-4.59: -3.89
< -5.30: -4.59

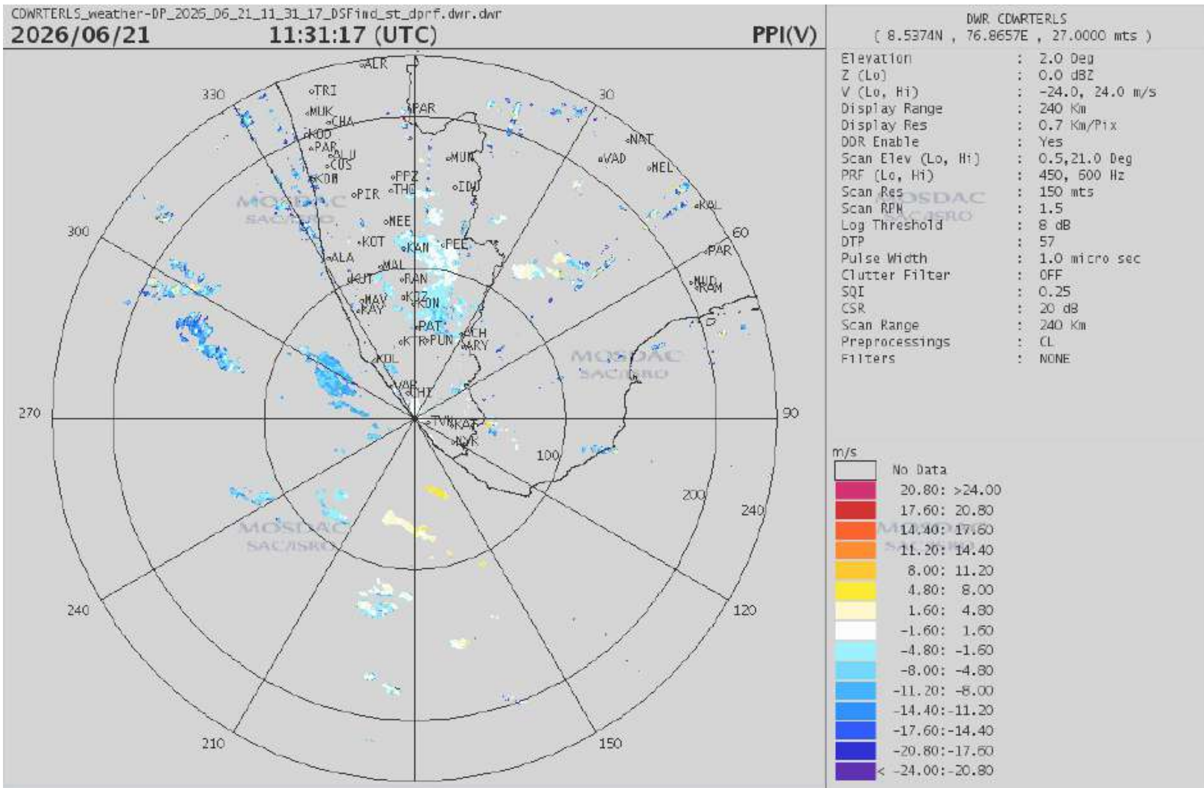
CDWRTERLS_weather-DP_2026_06_21_11_31_17_DSFind_st_dprf.dwr.dwr
2026/06/21
11:31:17 (UTC)
PPI(V)
DWR CDWRTERLS
(8.5374N , 76.8657E , 27.0000 mts)
Elevation : 2.0 Deg
Z (Lo) : 0.0 dBZ
V (Lo, Hi) : -24.0, 24.0 m/s
Display Range : 240 Km
Display Res : 0.7 Km/Pix
DDR Enable : Yes
Scan Elev (Lo, Hi) : 0.5,21.0 Deg
PRF (Lo, Hi) : 450, 600 Hz
Scan Res : 150 mts
Scan RPM : 1.5
Log Threshold : 8 dB
DTP : 57
Pulse Width : 1.0 micro sec
Clutter Filter : OFF
SQI : 0.25
CSR : 20 dB
Scan Range : 240 Km
Preprocessings : CL
Filters : NONE
m/s
No Data
20.80: >24.00
17.60: 20.80
14.40: 17.60
11.20: 14.40
8.00: 11.20
4.80: 8.00
1.60: 4.80
-1.60: 1.60
-4.80: -1.60
-8.00: -4.80
-11.20: -8.00
-14.40: -11.20
-17.60: -14.40
-20.80: -17.60
< -24.00: -20.80

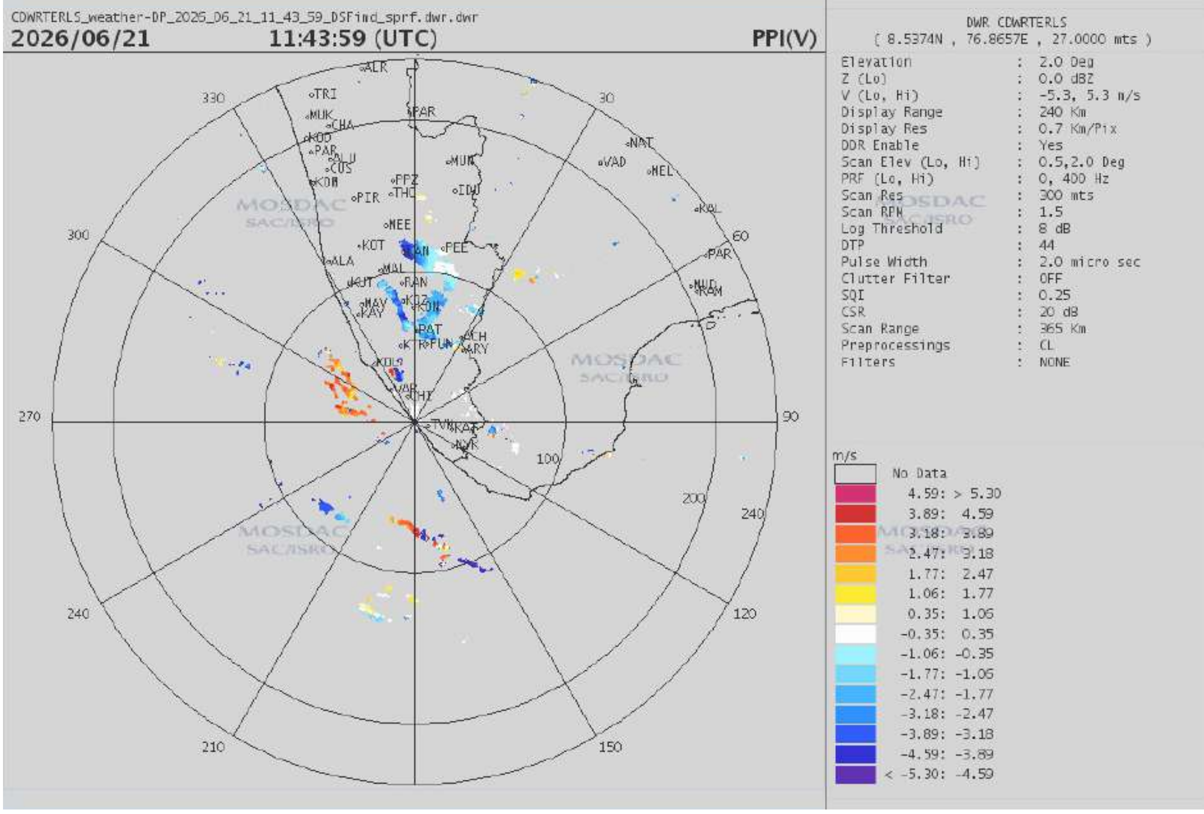
CDWRTERLS_weather-DP_2026_06_21_11_43_59_DSFind_sprf.dwr.dwr
2026/06/21
11:43:59 (UTC)
PPI(V)
DWR CDWRTERLS
(8.5374N , 76.8657E , 27.0000 mts)
Elevation : 2.0 Deg
Z (Lo) : 0.0 dBZ
V (Lo, Hi) : -5.3, 5.3 m/s
Display Range : 240 Km
Display Res : 0.7 Km/Pix
DDR Enable : Yes
Scan Elev (Lo, Hi) : 0.5,2.0 Deg
PRF (Lo, Hi) : 0, 400 Hz
Scan Res : 300 mts
Scan RPM : 1.5
Log Threshold : 8 dB
DTP : 44
Pulse Width : 2.0 micro sec
Clutter Filter : OFF
SQI : 0.25
CSR : 20 dB
Scan Range : 365 Km
Preprocessings : CL
Filters : NONE
m/s
No Data
4.59: > 5.30
3.89: 4.59
3.18: 3.89
2.47: 3.18
1.77: 2.47
1.06: 1.77
0.35: 1.06
-0.35: 0.35
-1.06: -0.35
-1.77: -1.06
-2.47: -1.77
-3.18: -2.47
-3.89: -3.18
-4.59: -3.89
< -5.30: -4.59

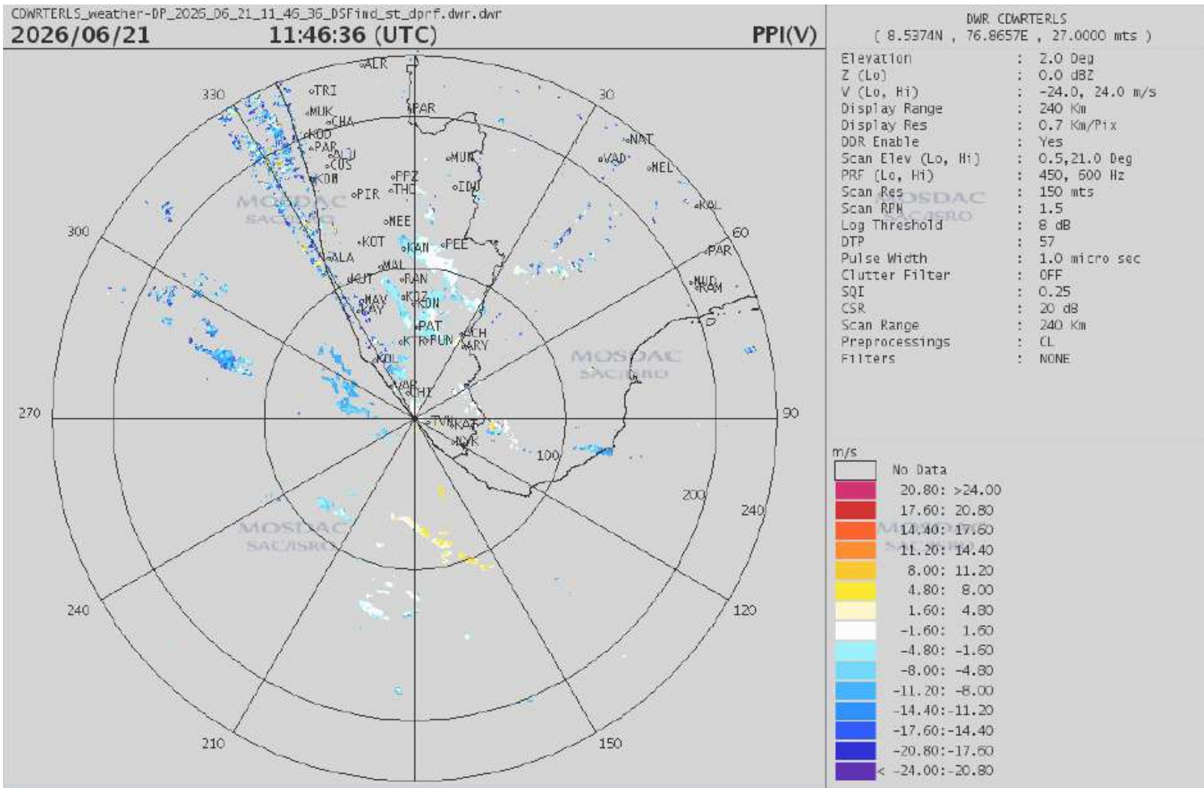
CDWRTERLS_weather-DP_2026_06_21_11_46_36_DSFind_st_dprf.dwr.dwr
2026/06/21
11:46:36 (UTC)
PPI(V)
DWR CDWRTERLS
(8.5374N , 76.8657E , 27.0000 mts)
Elevation : 2.0 Deg
Z (Lo) : 0.0 dBZ
V (Lo, Hi) : -24.0, 24.0 m/s
Display Range : 240 Km
Display Res : 0.7 Km/Pix
DDR Enable : Yes
Scan Elev (Lo, Hi) : 0.5,21.0 Deg
PRF (Lo, Hi) : 450, 600 Hz
Scan Res : 150 mts
Scan RPM : 1.5
Log Threshold : 8 dB
DTP : 57
Pulse Width : 1.0 micro sec
Clutter Filter : OFF
SQI : 0.25
CSR : 20 dB
Scan Range : 240 Km
Preprocessings : CL
Filters : NONE
m/s
No Data
20.80: >24.00
17.60: 20.80
14.40: 17.60
11.20: 14.40
8.00: 11.20
4.80: 8.00
1.60: 4.80
-1.60: 1.60
-4.80: -1.60
-8.00: -4.80
-11.20: -8.00
-14.40: -11.20
-17.60: -14.40
-20.80: -17.60
< -24.00: -20.80
MOSDAC
SAC/ISRO

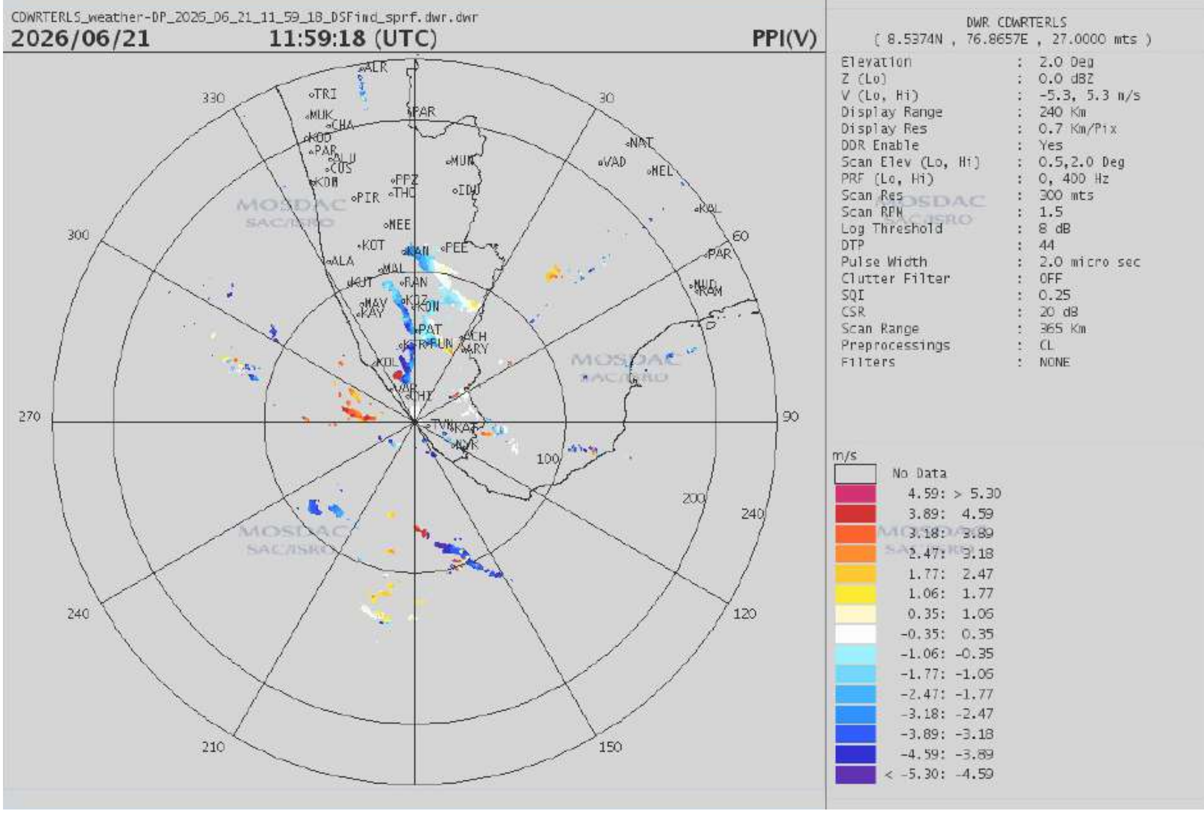
CDWRTERLS_weather-DP_2026_06_21_11_59_18_DSFind_sprf.dwr.dwr
2026/06/21
11:59:18 (UTC)
PPI(V)
DWR CDWRTERLS
(8.5374N , 76.8657E , 27.0000 mts)
Elevation : 2.0 Deg
Z (Lo) : 0.0 dBZ
V (Lo, Hi) : -5.3, 5.3 m/s
Display Range : 240 Km
Display Res : 0.7 Km/Pix
DDR Enable : Yes
Scan Elev (Lo, Hi) : 0.5,2.0 Deg
PRF (Lo, Hi) : 0, 400 Hz
Scan Res : 300 mts
Scan RPM : 1.5
Log Threshold : 8 dB
DTP : 44
Pulse Width : 2.0 micro sec
Clutter Filter : OFF
SQI : 0.25
CSR : 20 dB
Scan Range : 365 Km
Preprocessings : CL
Filters : NONE
m/s
No Data
4.59: > 5.30
3.89: 4.59
3.18: 3.89
2.47: 3.18
1.77: 2.47
1.06: 1.77
0.35: 1.06
-0.35: 0.35
-1.06: -0.35
-1.77: -1.06
-2.47: -1.77
-3.18: -2.47
-3.89: -3.18
-4.59: -3.89
< -5.30: -4.59
MOSDAC
SAC/ISRO

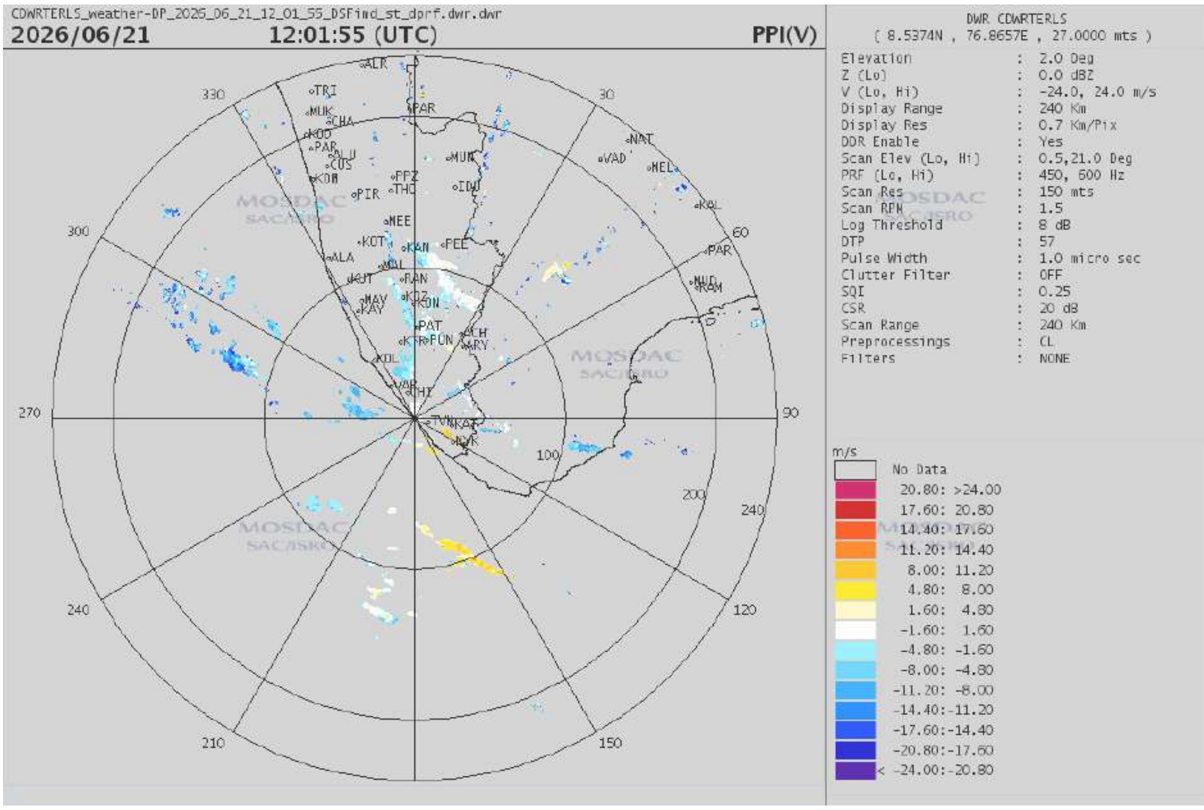
CDWRTERLS_weather-DP_2026_06_21_12_01_55_DSFind_st_dprf.dwr.dwr
2026/06/21
12:01:55 (UTC)
PPI(V)
DWR CDWRTERLS
(8.5374N , 76.8657E , 27.0000 mts)
Elevation : 2.0 Deg
Z (Lo) : 0.0 dBZ
V (Lo, Hi) : -24.0, 24.0 m/s
Display Range : 240 Km
Display Res : 0.7 Km/Pix
DDR Enable : Yes
Scan Elev (Lo, Hi) : 0.5,21.0 Deg
PRF (Lo, Hi) : 450, 600 Hz
Scan Res : 150 mts
Scan RPM : 1.5
Log Threshold : 8 dB
DTP : 57
Pulse Width : 1.0 micro sec
Clutter Filter : OFF
SQI : 0.25
CSR : 20 dB
Scan Range : 240 Km
Preprocessings : CL
Filters : NONE
m/s
No Data
20.80: >24.00
17.60: 20.80
14.40: 17.60
11.20: 14.40
8.00: 11.20
4.80: 8.00
1.60: 4.80
-1.60: 1.60
-4.80: -1.60
-8.00: -4.80
-11.20: -8.00
-14.40: -11.20
-17.60: -14.40
-20.80: -17.60
< -24.00: -20.80
330
30
300
60
270
90
240
120
210
150
100
200
240
MOSDAC
SAC/ISRO